

**SUBDOMINANT NEO-EPITOPES IN COMBINATION WITH
CHECKPOINT BLOCKADE MODULATORS ARE PROTECTIVE IN A
MODEL OF PANCREATIC ADENOCARCINOMA**

by
Heather L. Kinkead

A dissertation submitted to Johns Hopkins University in conformity with the requirements for
the degree of Doctor of Philosophy

Baltimore, Maryland
March 2017

© 2017 Heather L. Kinkead
All Rights Reserved

ABSTRACT

Pancreatic adenocarcinoma (PDA) remains one of the most lethal cancer types, with patients presenting with late-stage disease at time of diagnosis. Surgical resection, the only curative treatment, is limited to patients without metastases, a minority of those diagnosed. PDA is refractive to radiation and chemotherapy due to the dense stroma that is a hallmark of the tumor microenvironment. Despite the abundance of novel therapies available for other tumors, little progress has been made in the development of treatments for PDA. Immunotherapy in the form of induced adaptive immunity has the potential to infiltrate the tumor microenvironment and overcome the characteristic resistance mechanisms of PDA.

Mutations that arise during the development of PDA are specific to cancer cells and have therefore escaped the regulatory mechanisms that prevent cytolytic T cells from recognizing antigens that are also present on normal cells. Recent sequencing technology has allowed the genomic analysis of many cancers, including brain, breast, colorectal, ovarian, and pancreatic cancers. By targeting immunotherapy to the specific mutome of an individual tumor, a personalized treatment can be developed that is not limited by the presence of specific molecules involved with tumor cell proliferation, such as EGFR overexpression.

Therapeutic vaccines for tumor immunotherapy rely on activating immune effector cells, especially CD4⁺ helper T cells and CD8⁺ cytolytic T cells, capable of specifically recognizing epitopes expressed by tumor cell antigens. An obstacle has been identifying epitopes that are specifically recognized by tumor cells and not by normal tissues. Although genome-wide sequencing technologies have shown that human pancreatic cancer cells are not considered a hypermutated cancer and the tumor is not well infiltrated with effector T cells, this thesis shows that subdominant epitopes are capable of inducing an anti-tumor

response when coupled with appropriate immune-activating agents, including checkpoint blockade antibodies. Furthermore, we show that both unmutated and mutated tumor antigens can induce tumor-specific immunity, and that the addition of an agonist OX40 antibody fundamentally reprograms these effector cells to overcome tumor-induced exhaustion that synergizes with an anti-PD-1 antibody to provide near-complete, durable tumor rejection.

Advisor: Dr. Elizabeth Jaffee

Reader: Dr. Eric Lutz

Thesis Committee: Dr. Elizabeth Jaffee

Dr. Ivan Borrello

Dr. Leisha Emens

Dr. Eric Lutz

Dr. Vasanth Yegnasubramanian (Chair)

ACKNOWLEDGEMENTS

A critical component of a successful graduate school journey is a good mentor, and I was fortunate enough to have two. The encouragement, support, and guidance I received from Dr. Elizabeth Jaffee was paramount to the success of this project. I cannot possibly list everything you have taught me, but the one that stands out the most is how to tackle life with grace. There were some very difficult stretches, and I am forever grateful for your reassurance that everything would work out and that I would, in fact, graduate one day.

It was my honor to be the first graduate student for Dr. Eric Lutz. While the journey didn't end quite where we expected, his vision and experience were invaluable in shaping the project. I learned so much about immunology, how to develop a project, and what really good writing looks like, and I appreciate your sense of humor and determination throughout this process.

A good committee can help point you in the right direction, but a great committee teaches you how to find the right direction. I was privileged to have the latter. Dr. Leisha Emens has a unique talent for asking exactly the right question to make a story come together. Dr. Ivan Borrello provided not only great scientific mentorship but also adopted me as an unofficial lab member into his group. My chair, Dr. Vasan Yegnasubramanian, is one of the most talented scientists I have ever worked with. His creativity in approaching research is inspiring, and his endless enthusiasm for knowledge is contagious.

The members of my lab and of the 4th floor immunology group were critical in providing technical advice and moral support. In particular, I'm grateful for the scientific conversations and friendships of Susan Lee, Nina Chu, Alex Hopkins, Aggie Rucki, Rose

Parkinson, Kim Noonan, and Todd Armstrong. This long journey was made infinitely more interesting and fun by your presence.

Many thanks are due to my family, who have been there and supported me not just through graduate school, but also throughout my entire life. Even though there are thousands of miles between us, you always made sure that I knew I had somewhere to turn when I needed someone to listen and a little extra encouragement. To my mom, I appreciate the example you have set that it is never too late to chase your dreams. To my dad, I appreciate that while you nurtured my curiosity in science, you never pushed me to follow in your footsteps, letting me find my own journey. And to my sister, I am grateful for your endless encouragement.

To my husband, JT, none of this would have been possible without you. Your tireless patience, love, and support have been my foundation. I am so grateful to spend my life sharing in your adventures, and I am especially grateful that when I suggested leaving San Diego your immediate response was “let’s go.” There are no words to express how much I value your love and friendship.

TABLE OF CONTENTS

ABSTRACT.....	II
ACKNOWLEDGEMENTS.....	IV
LIST OF TABLES.....	VII
LIST OF FIGURES.....	VIII
CHAPTER ONE: Identifying targetable tumor epitopes.....	1
SUMMARY.....	1
INTRODUCTION.....	2
RESULTS.....	4
DISCUSSION.....	26
CHAPTER TWO: OPTIMAL ACTIVATION OF T CELLS FOR EFFECT TUMOR REGRESSION.....	28
SUMMARY.....	28
INTRODUCTION.....	29
RESULTS.....	33
DISCUSSION.....	56
REFERENCES.....	65
CURRICULUM VITAE.....	79

LIST OF TABLES

Table 1.1 Immunogenic epitopes identified by <i>in vivo</i> screening.....	7
Table 1.2 Validated immunogenic neoepitopes identified by whole-exome sequencing and <i>in vivo</i> screening.....	10
Table 1.3 List of immunogenic altered peptide ligands and mutant neoepitopes.....	13
Table 1.4 Minimal epitopes of immunogenic peptides.....	14
Supplementary Table 1.1.....	19
Table 2.1 Immunogenic Panc02 peptides used to test for antitumor efficacy.....	38
Table 2.2 Panc02 peptides used in R243 vaccine (STINGVac) checkpoint-blockade.....	45

LIST OF FIGURES

Figure 1.1 Screening of immunogenic epitopes	6
Figure 1.2 Panc02-specific neoepitopes are capable of inducing interferon-γ responses from CD8+ t cells.....	9
Figure 1.3 Responses to the immunogenic peptides are not primed by the tumor or by autologous GVAX.....	12
Figure 1.4 Mapped epitopes of immunogenic peptides.....	15
Figure 1.5 Immunization with some mutant neoepitopes and altered peptide ligands can induce cross-reactivity to the wild-type sequence.....	18
Figure 2.1 Induction of interferon-gamma in CD8+ T cells stimulated with Panc02 peptides.....	35
Figure 2.2 Panc02 peptides immunized with R243 and Addavax induces polyfunctional CD8+ T cells.....	36
Figure 2.3 Structure of the R243 STING agonist.....	37
Figure 2.4 Immunization with R243 and Panc02 peptides provides a survival benefit... 	39
Figure 2.5 Expression of exhaustion markers on tumor-infiltrating T cells.....	42
Figure 2.6 <i>In vitro</i> stimulation of Panc02 tumor cells by IFNγ results in surface PD-L1 expression.....	43
Figure 2.8 STING vaccine in combination with dual checkpoint therapy results in near-complete tumor protection.....	46
Figure 2.9 Average tumor diameter (mm) in STINGVac-treated mice with or without checkpoint blockade antibodies.....	48

Figure 2.10 Anti-OX40 augments STINGVac-primed T cells to maintain effector function in the tumor microenvironment.....	49
Figure 2.11 Anti-OX40 prevents the expression of exhaustion markers on tumor-infiltrating CD8+ T cells.....	51
Figure 2.12 Anti-OX40 and anti-PD-1 synergize with STINGVac to provide a durable anti-tumor response.....	53
Figure 2.13 Specificities of Panc02-reactive T cells from STINGVac, anti-OX40, anti-PD-1 treated mice.....	54
Figure 2.14 Tumor-infiltrating lymphocytes do not express cytokine with anti-CD3/28 stimulation.....	55

CHAPTER ONE: Identifying targetable tumor epitopes

Summary

Pancreatic ductal adenocarcinoma (PDA) is not considered a hypermutated cancer, with next-generation sequencing methods identifying an average of 63 mutations per tumor. Furthermore, with the exceptions of a few driver genes such as *KRAS*, *TP53*, *CDKN2A*, and *SMAD4*, these mutations are frequently patient specific. However, these novel mutations are not present in normal cells and provide a potential source of neo-epitopes for targeted immunotherapy. The success of this approach depends on establishing a strategy for singling out the most relevant targets for immunotherapy directly from sequencing data.

Several algorithms have been developed that predicted how well a peptide sequence will bind to major histocompatibility (MHC) molecules. These have shown some success in predicting which epitopes are likely to induce tumor-reactive T cells; however, it has become standard practice to prioritize mutations that are predicted to bind to MHC molecules with high affinity, typically less than 50 nM. By expanding our sample pool of epitopes to those that are predicted to have lower affinity binding to MHC molecules, we identified a pool of epitopes that were capable of inducing a robust CD8⁺ T cell response despite having only modest predicted affinity for MHCI. Furthermore, due to an error in the initial sequencing analysis, we are able to show that T cell responses can be induced to unmutated epitopes by immunizing with an artificially altered peptide sequence.

Introduction

Cancer cells accumulate tens to hundreds of somatic mutations during their development, collectively referred to as the cancer "mutome." The number of mutations varies between tumor types, with the highest mutations rates being observed in colorectal cancer with microsatellite instability (MSI-CRC), non-small cell lung cancer (NSCLC), and melanoma, and the lowest rates in blood and pediatric cancers (Vogelstein et al., 2013). A fraction of cancer mutations that occur in expressed genes are processed by the proteasome to generate novel peptides (termed mutant neoantigens) which are loaded onto major histocompatibility complex (MHC) molecules for T cell recognition. Mutant neoantigens provide ideal targets for immunotherapy because they arise from mutated gene products and are essentially foreign antigens that are presented only by MHC on the surface of tumor cells and not normal cells. Furthermore, as these neoantigens arise during tumor development, the T cell repertoire capable of recognizing mutant neoantigens with high avidity are not deleted by central tolerance. However, many tumor types have limited mutational landscapes with few neoantigens that are ideal targets for vaccine therapy. Additionally, neoantigens may have an effect on increased tumor antigenicity without being directly presented to effector T cells: these mutations may result in improved proteasomal processing, thereby increasing the amount of wild-type epitopes available for loading onto presentation molecules; they may improve translation, which would result in more transcript available for MHC presentation; or they may improve binding to major histocompatibility (MHC) molecules, allowing for priming of T cells that are specific for an unmutated epitope. This latter situation is not a unique feature of neoantigens and can be taken advantage of for priming of T cells reactive to tumor-shared antigens, using altered-peptide ligands.

There are several publicly-available algorithms that predict the affinity of an epitope for MHC molecules. These algorithms are limited in that they are only capable of predicting how well an epitope will bind to the presentation machinery, not how well a T cell receptor (TCR) will recognize a given epitope. However, it is unlikely that an epitope that does not bind stably to an MHC molecule would be able to trigger TCR signaling, allowing for activation of the epitope-reactive T cell. Many of the studies currently published use high affinity as a corollary for T cell reactivity. However, the epitope features important for binding to MHC molecules are not necessarily the same features that are required for T cell recognition. It is likely that there is some minimal threshold of binding to MHC that must be reached in order to trigger a T cell response, and that threshold has yet to be determined.

Results

Identification of tumor (neo)epitopes

Initial exome sequencing data was analyzed and found 596 non-synonymous, single nucleotide substitutions in the Panc02 cell line. For all mutations, candidate 8-11 amino acid-long neoantigens were predicted for H-2Kb and H-2Db using publically available major histocompatibility complex (MHC) class I epitope-binding prediction algorithms. The epitope binding prediction algorithms NetMHC3.2, NetMHC3.4, and NetMHCpan predicted that 245 mutations arising from non-synonymous single nucleotide substitutions would create epitopes capable of binding to either H-2Kb or H-2Db. Of these, 49 (8.2% of total mutations) were predicted to generate at least one neoantigen with an affinity for either H-2Kb or H-2Db of less than 50 nM by at least one algorithm and thus were considered strong binders. An additional 197 (33.1% of total mutations) were predicted to have an affinity of greater than 50 nM but less than 500 nM. Neoantigens were predicted in genes with functions both putatively related to oncogenesis, such as signaling and chaperone pathways, as well as in genes occurring in pathways likely unrelated to oncogenesis. Although screened by prediction algorithms, mutations occurring in unexpressed hypothetical proteins and splice junctions were excluded from *in vivo* screening. Long peptides were synthesized corresponding to 6 genes which contained mutations and were predicted to be oncogenic "driver" genes, as well as 25 mutated peptides not predicted to be immunogenic (affinity less than 500nM), in addition to the 132 mutated peptides predicted to be immunogenic (affinity greater than 500nM) for a final total of 169 peptides used for *in vivo* screening in the initial round. To increase the breadth of the screened mutome, we used an affinity of less than 1000 nM as the cutoff for predicted immunogenicity. The full list of screened mutations is shown

in **supplemental table 1.1**. This larger panel of epitopes was screened by IFN- γ ELISPOT to determine their ability to induce a CD8 $^{+}$ T cell response. Synthetic long peptides of greater than 15 amino acids have previously been used in immunization experiments to induce productive CD8 $^{+}$ T cell responses (Melief, 2009). We therefore created pools of 5 or 6 peptides (20 amino acids in length with the putative mutation at position 11) and immunized C57BL/6 mice with 10 μ g of each peptide (50 μ g total) in poly I:C as adjuvant as described in methods to test for the ability to induce interferon-gamma in CD8 $^{+}$ T cells (**Figure 1.1**). CD8 $^{+}$ T cells were isolated from splenocytes using negative selection, and evaluated for interferon-gamma production by ELISpot using the TAP-deficient cells lines T2-Kb and T2-Db as antigen-presenting cells (APCs, expressing class I MHC molecules from mouse), pulsed with 2 μ g/mL 20mer peptide. In total 23/163 (14%) peptides induced a measurable interferon-gamma response in (table 1), with 7 of these inducing a robust response (more than 100 spots per 100,000 CD8 $^{+}$ T cells). RNAseq was used to verify the expression of mutated genes and further refined this number to 14/124 (11%) expressed, immunogenic peptides derived from the Panc02 tumor cell line (**Table 1.1**).

After this initial screening, it was determined that many of the putative neoantigens previously identified were the result of errors in translating the genomic mutations to protein mutations and did not accurately reflect the non-synonymous single nucleotide substitutions present in the Panc02 cell line. Therefore, it was necessary to re-analyze the raw sequencing files to accurately determine the characteristics of the Panc02 genomic landscape. However, the previously identified immunogenic epitopes do reflect expressed genes in the Panc02 cell line, and the artificially introduced amino acid changes result in altered peptide ligands that

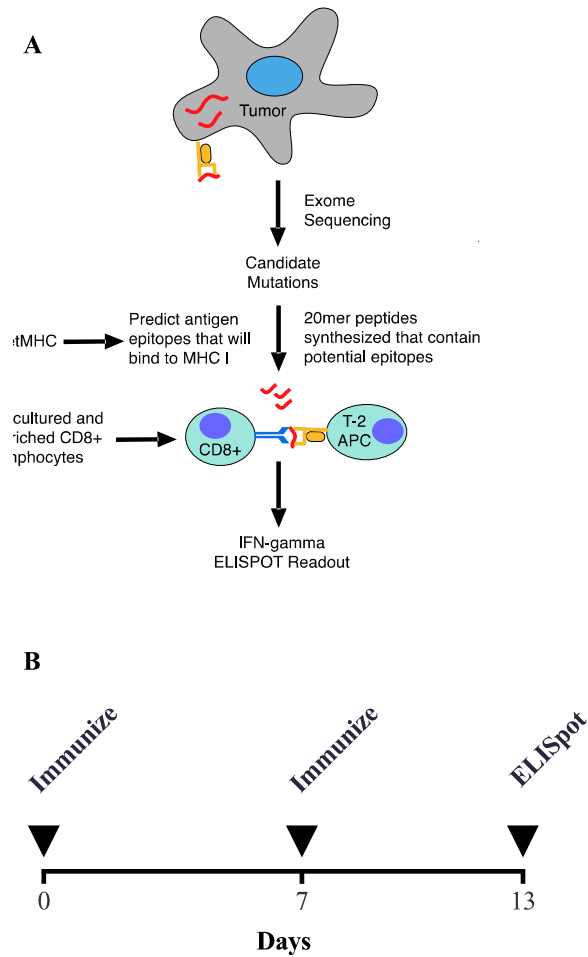


Figure 1.1 Screening of immunogenic epitopes

(A) Diagram of tumor neoepitope identification, from exome sequencing to *in vivo* verification.

(B) Schedule of immunizations for ELISpot analysis. Immunizations consisted of pools of 5-6 mutant Panc02 20mers + OVA 20mer combined with 10 μ g of poly I:C in AddaVax as adjuvants.

Table 1.1 Immunogenic epitopes identified by in vivo screening

Peptide Identifier	Mutant Gene	20mer Peptide Sequence
3	Olf1247	SLKTHSQEGRCKALSTCSSH
11	Slc5a9	WRRVCNINAITLLAINIFLW
14	Olf1549	CADIRVNVWYVLSVLLSTVV
20	Myo1g	LQGDVAFGHSNLFIRSPRTL
23	Ace	ALEKIAFLPFAYLVDQWRWG
35	Musk	WAYGVVLWEIVSYGLQPYYG
41	Slc17a6	GYIASRLAANPVFGAAILLT
43	Ankrd11	YAEYVTYTGSVLLDGKPLSK
44	Glb112	GSSAEESHLSCLNWSTLVPL
48	Gm10717	TFFSDFVIFQTFKWMFLIFL
51	Gm10715	RSYSVHFSFFKFFSDFVIFQ
53	Zfp955b	EDVAVNFSLGHWALLDSYQK
60	Ttc18	ASEMHFIFLRSGHIYLEEKE
66	Map2k5	MLWLALGPFCGMENQVLVIR
68	Olf1984	FRTFPMDKAVCVLYTMVTPM
74	Ampd1	QRFDKFNDKYSPVGASELRD
75	Zfp541	KMIQTKSVAQWVEYYYIWKK
77	Rasa3	TERIYSLFNLSMGKLEKMQE
84	Cln7	ALGLRHLVVVGNGHNQVVGLV
94	Notch2	AELINCQADVSAVDDHKGSA
133	Kcnj12var2	DGKLCLMWRVANLRKSHIVE
135	Ktn1var3	WISEKEKEITGLCNELESLK
156	Rnf26	FTFGGLQALGALLYSCYSGL

Peptide identifier and sequences for the initially identified 23 immunogenic Panc02 peptides

may have improved T cell priming capabilities compared to the wild-type sequences, therefore these epitopes were not excluded from immunogenicity studies. The raw sequencing files were aligned to the mm9 reference genome using bowtie2 (Langmead, Salzberg, 2012), variants were called using freebayes (Garrison, Marth, 2012) and then subsequently annotated using Annovar (Wang et al., 2010). Mutome-specific peptide sequences were extracted using R (R Core Team, 2016) and then analyzed by a locally-maintained NetMHC3.4 software package (Lundegaard et al., 2008). All mutated epitopes predicted to bind to either H-2-Kb or H-2-Db with an affinity of less than 1000 nM were manually curated by the Integrated Genomics Viewer (IGV) (Robinson et al., 2011; Thorvaldsdottir et al., 2013). The full pipeline is available on the git repository: https://github.com/rosgood/Panc02_Variant_ID.git.

From this most recent analysis of the Panc02 exome sequencing, 878 non-synonymous mutations were identified, with 269 of these predicted to bind either H-2-Kb or H-2-Db with an affinity of less than 1000 nM. 150 mutations were in expressed genes, and 48 of these had been previously screened for *in vivo* immunogenicity. After validating each mutation in IGV and removing mutations present in the mouse mm9 dbsnp database (Waterston et al., 2002), 70 novel mutations were identified that were predicted to bind to mouse H-2-Kb or H-2-Db. These were screened for the ability to induce interferon-gamma responses in isolated CD8⁺ T cells as well as in whole splenocyte fractions (**Figure 1.2**). ELISpot analysis of mice immunized with pools of 5 peptides (following the schedule in **Figure 1.1**), using Ova₁₅₂₋₁₇₁ as a positive control revealed 15/70 (21%) peptides to be immunogenic (**Table 1.2**) Interestingly, immunization with 2 of these peptides resulted in interferon-gamma responses only when whole splenocytes were pulsed with peptide, but not

IFN γ Producing CD8⁺ T cells

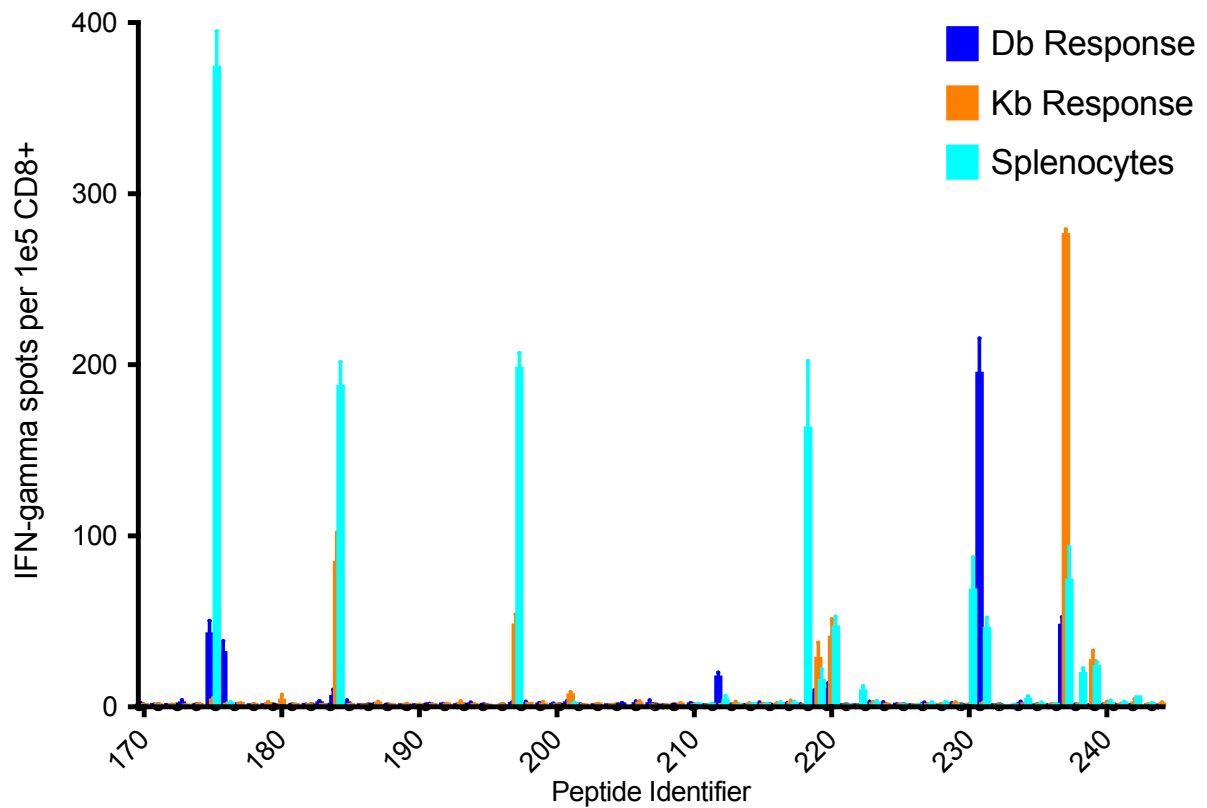


Figure 1.2 Panc02-specific neoepitopes are capable of inducing interferon- γ responses from CD8⁺ t cells

Immunization with 20mer peptides corresponding to mutant Panc02 peptides was performed according to **Figure 1.1B**. Peptide identifier is defined in **Table 1.1**. Isolated CD8⁺ T cells were stimulated overnight with T2 APCs pulsed with cognate peptides on an interferon- γ capture plate and resulting spots counted. Each bar represents the mean of triplicate wells \pm SEM.

Table 1.2 Validated immunogenic neoepitopes identified by whole-exome sequencing and *in vivo* screening

Peptide Identifier	Protein:mutation	Peptide Sequence	Best Predicted Epitope	Predicted Affinity (nM)
175	Bsg:p.A8P	MAAALLLPLAFTLLSGQ	LPLAFTLL	425
176	Ccdc67:p.N186T	KCSQFQKQAQTYQTQLNGKK	QAQTYQTQL	857
184	Cwc22:p.G507A	AQQRTYEKFFALLAGRFCML	RTYEKFFAL	33
197	Hmcn1:p.C2362W	VHVSDTGRYVWVAVNVAGMT	YVWVAVNV	955
201	Kansl1:p.P129A	ELRAELLGRQAVLEFSLENL	AVLEFSLENL	816
212	Ndufs6:p.V4A	MAAALTFRRLTL	AALTFRRL	59
218	Pnpla7:p.W1153C	LSGWLLWKRCNPLATKVKV	LLWKRCNPL	435
219	Ppp2r3a:p.T197I	SHRNSLDTNLISMLFQNLSE	ISMLFQNL	2
220	Prkcb:p.E449Q	KEPHAVFYAAQIAIGLFFLQ	AVFYAAQI	441
222	Rimbp3:p.G685V	KEMQGLQFQPVHPSETSETT	QGLQFQPV	103
230	Tg:p.R2226L	KVGTAWKQVYLFLGVPYAAP	QVYLFLGV	12
231	Tmem30c:p.L169I	ANSIFNDTITISYNLNSSTQ	NSIFNDTITI	125
237	Ttn:p.E19018A	IKIVRLTTGSAYQFRVCAEN	SAYQFRVC	31
238	Tubg1:p.G143W	EGFVLCHSIAWGTGSGGLGSY	IAWGTGSGL	621
239	Usp19:p.P829S	VQQRQPVPISISISKCAACQR	ISISKCAAC	862

when isolated CD8⁺ T cells were stimulated with the T2 APC, indicating either CD4⁺ T cell reactivity (as T2 cells do not express class II MHC molecules from mouse and therefore cannot stimulate a CD4⁺ response) or a deficiency in processing the 20mer peptide for MHCI presentation by the T2 cell line. When CD8⁺ T cells are isolated from mice either treated with autologous GVAX (as described in methods) or bearing Panc02 tumors, no detectable responses are seen to the identified epitopes, indicating that these are not dominant epitopes from the Panc02 tumor (**Figure 1.3**). A complete list of immunogenic epitopes, including the identified altered-peptide ligand epitopes, is available in **Table 1.3**.

Epitope Mapping

To further characterize the identified immunogenic epitopes, mapping experiments were performed. For the identified immunogenic neo-epitopes, it would be expected that the mutated residue could either be recognized directly by the TCR, or that it would improve recognition of the native peptide sequence by improved presentation, either by improved MHCI binding or by improved loading onto MHCI molecules. The altered-peptide ligands (identified in screen 1, which reflect unmutated, expressed tumor sequences) are expected to improve recognition of the native peptide sequence, therefore it would be expected that the altered amino acid from the immunizing peptide would likely fall in an anchor position when mapped. Exact peptides of the immunogenic peptides were synthesized for all epitopes 8-11 amino acids in length for all epitopes predicted to bind with less than 1000 nM affinity (**Table 1.4**). Mice were immunized with 20mer peptides as before, and then ELISpot analysis was performed using T2 cells pulsed with either the 20mer immunization peptide or the appropriate minimal epitope(s). ELISpot results are shown in **Figure 1.4**. In some cases,

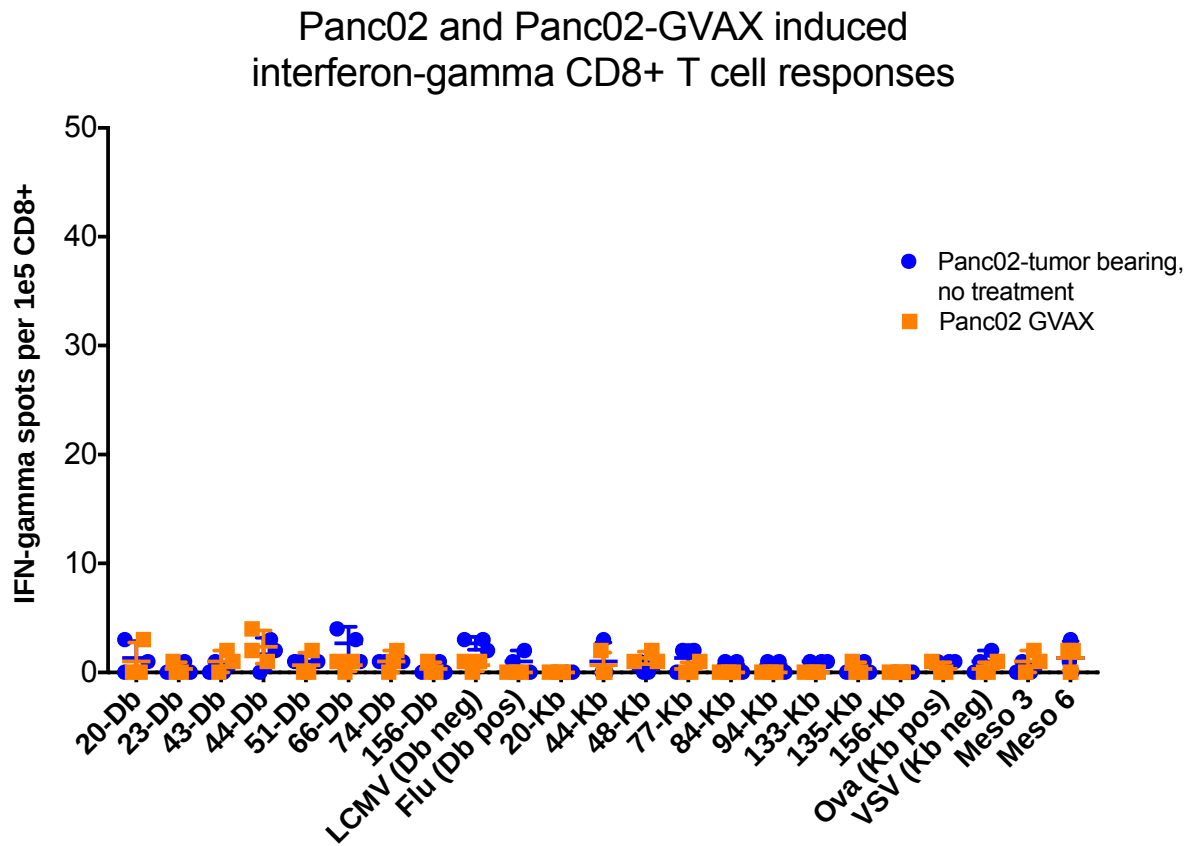


Figure 1.3 Responses to the immunogenic peptides are not primed by the tumor or by autologous GVAX

Mice were primed with 2 doses of GVAX given in 3 limbs, while Panc02 tumor-bearing mice received no treatment. Peptide identifier (as defined in **Table 1.1**) is shown with the T2 APC MHC restriction. Symbols represent each replicate with a line at the mean \pm SEM.

Table 1.3 List of immunogenic altered peptide ligands and mutant neopeptides

Peptide Identifier	Mutant Gene	20mer Peptide Sequence	Altered peptide ligand (APL)?
3	Olf1247	SLKTHSQEGRCKALSTCSSH	
11	Slc5a9	WRRVCNINAITLLAINIFLW	
14	Olf1549	CADIRVNVWYVLSVLLSTVV	
20	Myo1g	LQGDVAFGHSNLFIRSPRTL	
23	Ace	ALEKIAFLPFAYLVDQWRWG	
35	Musk	WAYGVVLWEIVSYGLQPYYG	
41	Slc17a6	GYIASRLAANPVFGAAILLT	
43	Ankrd11	YAEYVTYTGSVLLDGKPLSK	APL
44	Glb112	GSSAEESHLSCLNWSTLVPL	APL
48	Gm10717	TFFSDFVIFQTFKWMFLIFL	
51	Gm10715	RSYSVHFSFFKFFSDFVIFQ	
53	Zfp955b	EDVAVNFSLGHWALLDSYQK	APL
60	Ttc18	ASEMHFIFLRSGHIYLEEKE	APL
66	Map2k5	MLWLALGPFCGMENQVLVIR	
68	Olf1984	FRTFPMDKAVCVLYTMVTPM	
74	Ampd1	QRFDFKNDKYSPVGASELRD	
75	Zfp541	KMIQTKSVAQWVEYYYIWKK	
77	Rasa3	TERIYSLFNLSMGKLEKMQE	APL
84	Cln7	ALGLRHLVVVGNNHNVVGLV	
94	Notch2	AELINCQADVSAVDDHGKSA	APL
133	Kenj12var2	DGKLCLMWRVANLRKSHIVE	
135	Ktn1var3	VISEKEKEITGLCNELESLK	
156	Rnf26	FTFGGLQALGALLYSCYSGL	
175	Bsg	MAAALLPLAFTLLSGQ	
176	Ccdc67	KCSQFQKQAQTYQTQLNGKK	
184	Cwc22	AQQRTEYKFFALLAGRFCML	
197	Hmcn1	VHVSDTGRYVWVAVNVAGMT	
201	Kansl1	ELRAELLGRQAVLEFSLENL	
212	Ndufs6	MAAALTFRRLTL	
218	Pnpla7	LSGWLLWKRCNPLATKVKV	
219	Ppp2r3a	SHRNSLDTNLISMLFQNLSE	
220	Prkcb	KEPHAVFYAAQIAIGLFFLQ	
222	Rimbp3	KEMQGLQFQPVHPSETSETT	
230	Tg	KVGTAWKQVYLFLGVPYAAP	
231	Tmem30c	ANSIFNDTITISYNLNSSTQ	
237	Ttn	IKIVRLTTGSAYQFRVCAEN	
238	Tubg1	EGFVLCHSIAWGTGSGGLGSY	
239	Usp19	VQQRPPQVPSISISKCAACQR	

Table 1.4 Minimal epitopes of immunogenic peptides

Peptide Identifier	Protein:mutation	Minimal epitope	Predicted affinity (nM)
20	Myo1g:p.K696N	VAFGHSNL	7
20	Myo1g:p.K696N	VAFGHSNLF	10
20	Myo1g:p.K696N	VAFGHSNLFI	177
23	Ace:p.G473A	KIAFLPFAYL	387
23	Ace:p.G473A	IAFLPFAYLV	390
44	Glb1l2:pG36C	LSCLNWSTL	632
44	Glb1l2:pG36C	SCLNWSTLV	844
66	Map2k5:p.A11G	CGMENQVLV	380
66	Map2k5:p.A11G	LALGPFCGM	427
66	Map2k5:p.A11G	CGMENQVLVI	897
77	Rasa3:p.T203S	RIYSLFNL	20
77	Rasa3:p.T203S	RIYSLFNLSM	391
77	Rasa3:p.T203S	LSMGKLEKM	395
77	Rasa3:p.T203S	SLFNLSMGKL	564
77	Rasa3:p.T203S	FNLSMGKL	931
77	Rasa3:p.T203S	IYSLFNLSM	969
84	Clcn7:p.D771G	VVVGHNHNQV	256
175	Bsg:p.A8P	LPLAFTLL	425
175	Bsg:p.A8P	LLPLAFTLL	643
237	Ttn:p.E19018A	SAYQFRVC	31
237	Ttn:p.E19018A	SAYQFRVCA	437
237	Ttn:p.E19018A	SAYQFRVCAE	973
239	Usp19:p.P829S	ISISKCAAC	862

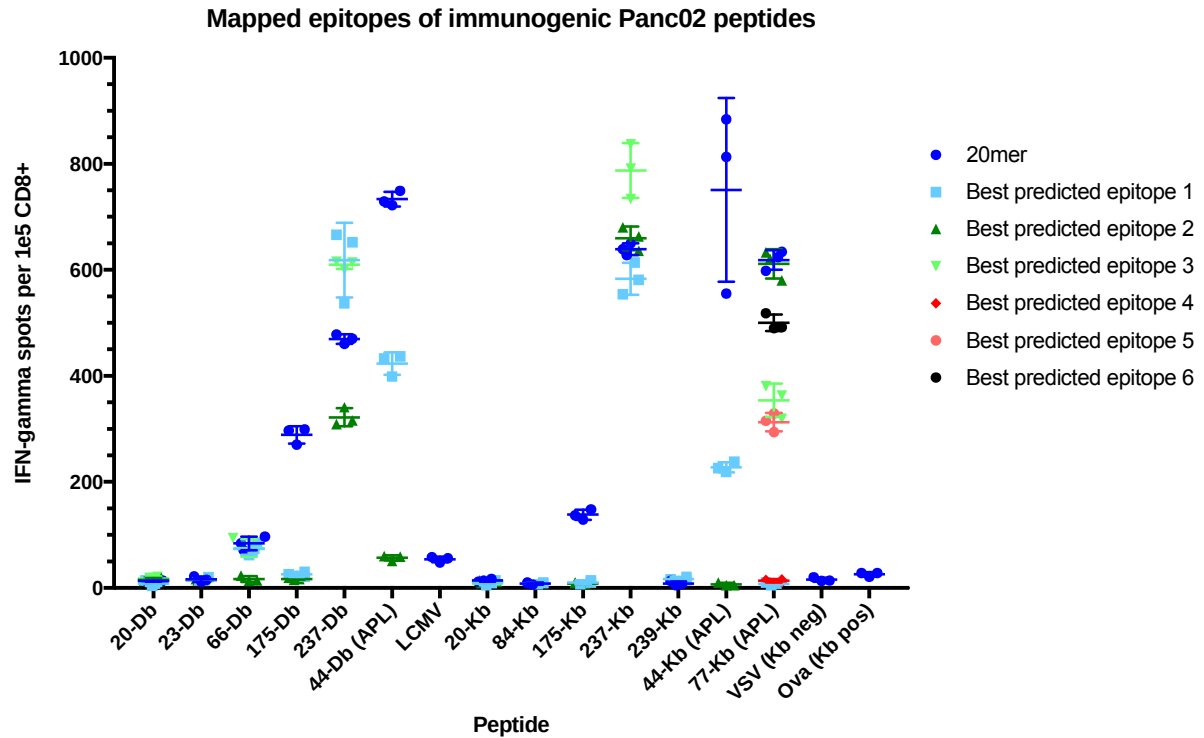


Figure 1.4 Mapped epitopes of immunogenic peptides

Mice were immunized with pooled 20mer peptides and isolated CD8⁺ T cells were tested for reactivity to the minimal epitope. Epitope sequence are listed in **Table 1.4** and are ordered according to their predicted affinity. Altered peptide ligands are marked as “(APL)” after the peptide identifier and MHC-restricted allele. Symbols represent each replicate with a line at the mean \pm SEM.

multiple minimal epitopes were capable of inducing interferon-gamma responses at the same level or better than the 20mer immunizing peptide, indicating that the responding T cells may recognize multiple epitopes (particularly where the different epitopes only differ by the addition of one amino acid at the C-terminal end of the epitope) and each epitope screened is sampling the same pool of responsive peptides, while in other cases there are several minimal epitopes that induce a response, but not at the same level as seen with the 20mer. This could be because the number of T cells responding to stimulation with the 20mer peptide represents the whole peptide responsive repertoire, and each minimal epitope represents a fraction of that repertoire. There are some immunogenic peptides that have not yet been tested and in some cases we did not see robust responses to the immunizing peptide, so these experiments will be repeated. Furthermore, there are some examples where there was a strong response to the immunizing peptide, but no response was seen to the minimal epitopes, indicating that the epitope responsible for inducing the CD8⁺ T cell response is not predicted to bind to MHCI and has yet to be identified.

Cross-reactivity to native peptide sequences

Non-synonymous mutations may induce tumor-reactive T cells by presentation of the mutation to the T cell receptor, in which case it would be recognized as a foreign epitope; by increasing the affinity for the MHCI molecule, in which case the mutation provides an optimal anchor residue; or by improving epitope production, either by introducing an improved sequence for proteasomal cleavage or TAP-mediated MHC loading. In the first instance, tumor-reactive T cells would not be deleted through central tolerance mechanisms because the epitope exists only within the tumor, similar to a foreign antigen. In the second

and third instances, the native epitope may not bind MHC with strong enough affinity to activate a naïve T cell (but could trigger TCR signaling in a primed T cell) and therefore wouldn't necessarily trigger thymic deletion, or reactive T cells escaped thymic deletion. For the identified neo-epitopes, cross-reactivity to native epitopes would not determine the anti-tumor efficacy of the vaccine, but for the altered-peptide ligand epitopes, it would be expected that cross-reactivity to native epitopes would be a requirement for anti-tumor efficacy. To determine the cross-reactivity to the native peptide sequences, mice were immunized with the neoantigen peptides and altered peptide ligands according to the schedule in figure 1, and ELISpot assays were performed using T2 APCs pulsed with either the corresponding 20mer native peptide or the mutant 20mer peptide and resulting interferon-gamma responses from isolated CD8⁺ T cells were analyzed (**Figure 1.5**). While only a few of the selected epitopes were tested for ability to induce a cross-reactive response, the three altered peptide ligands tested were able to induce similar levels of interferon-gamma with either the altered peptide or the native peptide. However, only one of the nine neoantigen peptides tested was capable of inducing a cross-reactive response, despite robust responses to the mutant peptide.

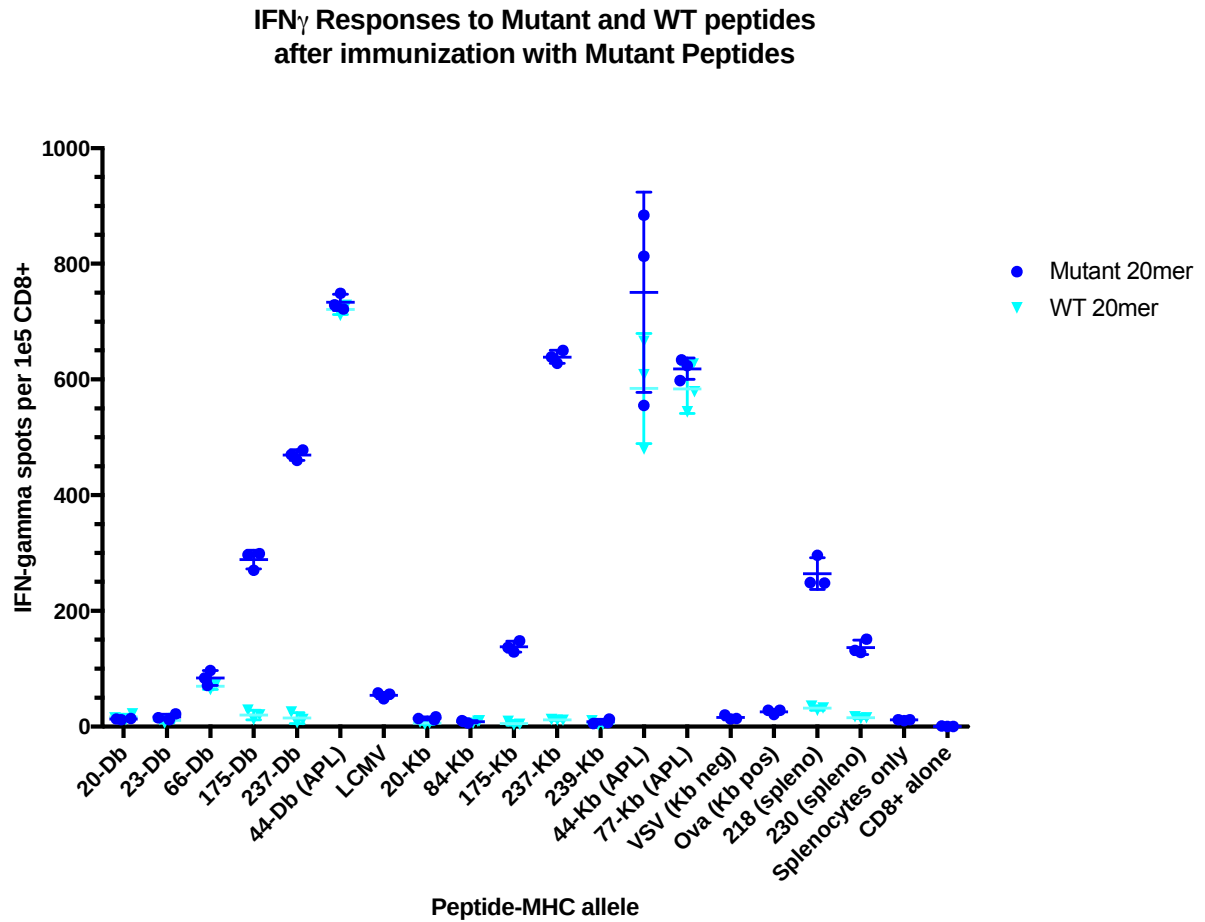


Figure 1.5 Immunization with some mutant neopeptides and altered peptide ligands can induce cross-reactivity to the wild-type sequence

Mice were immunized with pooled 20mer peptides corresponding to the mutant neopeptides and altered peptide ligands, and isolated CD8⁺ T cells were analyzed for cross-reactivity to the wild-type 20mer. Altered peptide ligands are marked as “(APL)” after the peptide identifier and MHC-restricted allele. Symbols represent each replicate with a line at the mean \pm SEM.

Supplementary Table 1.1

Peptide Identifier	Gene Name	20mer Peptide Sequence	Mutation
1	Olfr1136	LIRMDPQLHIAMYFFLSHLS	P58A
2	Olfr1217	FANSGAICILFSLLLVSYG	I209L
3	Olfr1247	SLKTHSQEGRCKALSTCSSH	R232C
4	Olfr1278	TEMVLLVAMALDRYVAICKP	W120L
5	Gatm	ISTIKVNIRNGNSLGGGFHC	A398G
6	4833422F24Rik	LFLGLLGESVWYLHRYLTD	A241V
7	Fat4	RRPLPSPSLWQLLRVWGLL	C22W
8	Chrn2	VSYDGSIFWLLPAIYKSACK	P147L
9	Hsd3b3	SNTIHKALKNNFILRGGGKS	K154N
10	Ptgr1	EYVTEGF EKMAAAF MGMLKG	P310A
11	Slc5a9	WRRVCNINAITLLAINIFLW	I672T
12	Niacr1	NCDIYSSVDLPFFTLSFTY	A272P
13	Emid2	CRWPGPCANLMSYRTLIRPT	V93M
14	Olfr549	CADIRVNVWYVLSVLLSTVV	G201V
15	Odz3	SLVTGDYLYNVSYSDNDNDVT	F1561V
16	Fam92b	EARPLTDTNPPPSVPWPLAS	A241P
17	Bcl2a1d	TCLQTSFQFWTRIHNE	G123T
18	Olfr770	TTLFCVVLSYAYIIKTILKF	V215A
19	Olfr806	LITEFYLLAALSVDRYVAIC	M116L
20	Myo1g	LQGDVAFGHSNLFIRSPRTL	K696N
21	Kcnj12	MVEATAMTTQPRSSYLANEI	A312P
22	Cacnb1	LTSLRRLNSFCGGLEASPRG	W503C
23	Ace	ALEKIAFLPFAYLVDQWRWG	G473A
24	Stab1	IHKANYIAANRVFHTVTALR	G486R
25	Pfkm	MNNWEVYKLLSHVRPPVSKG	A389S
26	Olfr121	SLSVKRFAFATFSEVPGECF	K22T
27	Gpr111	PVLHHNGCVATTFVHFFYL	A456T
28	Arhgap28	AVMLKAFFREMPTSLFPVEY	L470M
29	Fhod3	EKEDKLSERVTGLWSTSLQ	A809V
30	Slc6a7	GSQSPKPLMVNMRKYGGITS	H607N
31	Supv3l1	YTTGEEVEVQTYERLTPISV	K344T
32	Dnahc9	PAVKQSISKFI AFVHISV NK	M3013I
33	Daam2	LRQHENAILDTHLDFEMVR	K326T
34	Vps39	KANSPLKGHEWTVQYLQHLG	R538W
35	Musk	WAYGVVLWEIVSYGLQPPYG	F797V
36	Rimbp2	VHLCVARYSYTPFDGPNENP	N200T
37	Mug1	QASSVEVEMNIYVVLARLTA	R1187I
38	Abcc9	DATVTEGGENISVGQRQLFC	F1446I

Supplementary Table 1.1 (continued)

Peptide Identifier	Gene Name	20mer Peptide Sequence	Mutation
39	Supt5h	VVTVRHQAVTLKKDNRFAVA	Q575L
40	Zfp940	VNQGIVFNNHKRLNAGEKAT	Q159K
41	Slc17a6	GYIASRLAANPVFGAAILLT	R153P
42	Smg1	GENTYGRKSLVQELRINNV	G103V
43	Ankrd11	YAEYVTYTGSVLLDGKPLSK	L2456V
44	Glb1l2	GSSAEESHLSCLNWSTLVPL	G36C
45	Slc6a20a	LLIVLVETIANCYVYGLKRF	K430N
46	Muc6	IFTATCGDDVAATFSIQLRR	P80A
47	A330008L17Rik	SPVRWISKPGFFFFLLQV	C81F
48	Gm10717	TFFSDFVIFQTFKWMFLIFL	K213T
49	Gucy2d	SVLSVFWWSVRLWADSLSLL	L53R
50	Gm10647	FCLFCFVVFVSQAPSDYHRV	G88S
51	Gm10715	RSYSVHFSFFKFFSDFVIFQ	T200K
52	Gm10719	DFVIFQVVKWMFLIFLDFQF	K214M
53	Zfp955b	EDVAVNFSLGHWALLDSYQK	P23H
54	Gm14403	LDPSQKSLYKDVMLETHRNL	G31D
55	Gm11168	VCISHFSRFSLISSFFKSSS	V67L
56	Gm904	TIGFMCVGVLFLIPFLKE	F38L
57	Heph1l	MHAVNGYMYGIQPLSMCKK	S63OI
58	Col6a5	SDALHNEFQLCTFKNRNPML	G85C
59	Irg1	EHEARHSFQYMACASLLDGS	V338M
60	Ttc18	ASEMHFIFLRSGHIYLEEKE	N982S
61	Btnl4	FSFHEASFSGSLFPYFRLKS	T490S
62	Zfp423	KKAEFIKGSHMCNVCSTRTFF	K939M
63	Gpr125	SGNLFTSLSQATFDYLGSLR	G160A
64	Kcnq3	YDALERPRGWLLYHALVFL	R120W
65	Olfr151	TAFMYLKPSTISSLAQENVA	L264I
66	Map2k5	MLWLALGPFCGMENQVLVIR	A11G
67	Ros1	EITQVFSNISRTMLNPPELQ	G627R
68	Olfr984	FRTFPMDKAVCVLYTMVTPM	S272C
69	Gtf2ird2	YEQMLQDEAAMVVRGLPEGL	V140M
70	Olfr1356	PFIYSLRNKDTQKALGKLLR	M297T
71	Cts3	SAVASLGPISFVIDAWHESF	V244F
72	Vmn1r235	KTILLQLSTFILCYIISCLF	M264I
73	Scn9a	CKLSDFAAALTPELLIAKPN	A1797T
74	Ampd1	QRFDKFNDKYSPVGASELRD	N378S
75	Zfp541	KMIQTKSVAQWVEYYYIWKK	C1209W
76	Tpcn2	ITLWNVMVVNTWQVILEAYK	N637T

Supplementary Table 1.1 (continued)

Peptide Identifier	Gene Name	20mer Peptide Sequence	Mutation
77	Rasa3	TERIYSLFNLSMGKLEKMQE	T203S
78	Lactb	LGLALGAKLVFGLRGAVPIQ	V58F
80	Fam75d3	YQGLTKAYAVTPGDHLSPSP	A221T
81	Utp20	LTNVFAVLSAENLSEATASI	K1243E
82	Cant1	TGSRAQEENTLFSYLKKGYL	W127L
83	Cblb	YELYCEMGSTLQLCKICAEN	F370L
84	Clcn7	ALGLRHLVVVGNNHNVVGLV	D771G
85	Cnppd1	NDEWGAAGGVTVATLNALER	A155T
86	Fbf1	FSSSLNTLSSLVEASHLTTS	R798L
87	Gkap1	VLSSVLTASP FALLQVDSG	R15P
88	Irf7	YTETLLQHVS PGLQELRGP	T277P
89	Jak1	YDPNQRPFFR DIMRDINKLE	A839D
90	Ktn1	VISEKEKEITYLCNELESLK	D986Y
91	Mars	SAICRYFFLLWGWEQDDL TN	C73W
92	Mmp10	DPALSFDSVSM LRGEVLFFK	T300M
93	Mocs3	LSRDEILRYSPQLLLPELGV	R65P
94	Notch2	AELINCQADVSAVDDHGKSA	A1969S
95	Pik3r5	EEEEDELEMDRYCAERDSLLS	H333Y
96	Ptpn11	TIQMVRSQRSVMVQTEAQYR	G507V
97	Rbm5	TALSPYASLAINNIRLIKDK	V259I
98	Rhpn2	VHFLDPHCSALLAGAKEGDY	S548L
99	Rrs1	QAKKERVAKNVNLRNLAR	A194V
100	Slc16a13	FFIPYVHLVANLQDLGWDPL	H240N
102	Slc35b3	NLTGVMLISLPLCADA VIGN	A203P
104	Syncrip	ISVANNRLFVASIPKSKTKE	G248A
105	Tm7sf3	YNFFETTIKFTPANIGYARA	A160T
106	Ubqln1	ASMFNTPGMQALLQQITENP	G12A
107	Vprbp	PVSLPRTPRIGNGIASRLGS	A905G
108	Zbtb43	MAHRRWIHV KPERLEQAWDG	A248P
109	4933409G03Rik	GGDDEDGGDEYGGDGGGDD	D122Y
110	Acsm2	ASLTMHHLWKHPRLFTLWGN	P32H
111	Actr8	ELWIYQREWQHFGVRMLRER	R610H
112	Ankrd11var2	GHKSLCVNEVLSFYVPMVDV	W2625L
113	Arhgap30	HPVVPLVAPQSQTAFETQT	R1076S
114	Arvcf	KRRVRQLRGLSLLVALLDHP	P405S
115	Baz2a	SIFVSPTSPRLGESVLQDN	G373R
116	C2cd3	TSPWSSFMSDLSEVLSPQPT	M2073L
117	Ccdc113	DIKITAAEF SKLRSRRKSKA	Q76K

Supplementary Table 1.1 (continued)

Peptide Identifier	Gene Name	20mer Peptide Sequence	Mutation
118	Ccdc67var2	LKAQFSKLTSTFEKRLRHQM	N106T
119	Cpa4	LLDNEDEEMQNNEGIERSGD	H107N
120	Csn3	RSVLNFNQYERNYYHYRPSL	P60R
121	Daglb	TDLVPSDIAACFTLLHQQQD	G238C
122	Dip2bvar2	SEGETVVNVLFHKDAGLWH	D324H
123	Dip2b	ERIASVLGDKAHLNAGDNVV	G805A
124	Emilin2var2	AEPSQLPGIPCSKESGMKDI	S258C
125	Fam83c	TLGHSKLDLIAKYHQLQGAR	T710A
126	Frmd6	RGKDYILKHIQNMHKDQFAL	P201Q
127	Fxr2	PQRRNRSRRRCNRGNRTDGS	R594C
128	Fzd9	AMEIPMCRGIVYNLTRMPNL	G52V
129	Gm10564	RAGRDVEPRARATRRDWEPR	S154R
131	Hdgfrp3	QSRKSPGDEDGKDCKEEENK	D167G
132	Itpr3	EEPGGKNVRRFIQGVGHMMS	S916F
133	Kcnj12var2	DGKLCLMWRVANLRKSHIVE	G216A
134	Klhl7	ISKNFLSKTVLAEPLIQDNP	Q248L
135	Ktn1var3	VISEKEKITGLCNELESLK	D986G
136	Lonrf1	YLEDVKIENGNEIRSLRELH	D739N
137	Lrnf1	APTLTMLCAKMGLLFVPPAI	T54M
138	Lrrc66	GMWQPQSPVELIDSQDEQVTD	R351I
139	Lrrcc1var2	QNMDDAFRRQGDEIVEAHQA	V958G
140	Lrrcc1	QNMDDAFRRQMDEIVEAHQA	V958M
141	Mbtd1	ITAIKKQNILYNPKEKADWF	H12Y
142	Mtap2	YYKNGTVMAPGLPEMLDLAG	D807G
143	Mybbp1a	MKYALKRLITALGVGREAR	G78A
145	Otop1	SQHQKMQCRFYGVLVGSVLG	D307Y
146	Paip1var2	RAPEQTKPQRDPPSSQDKIP	A17D
147	Pion	LVLHLNSHCSSADFEVFHLM	A675S
148	Ppig	KERDHETTKETEKPLDPKGK	K499T
149	Prdm16	VSNSSQGATAPTGSEEKFDG	A573P
150	Prkcb	DLTSRNDFMGFLSFGISELQ	S258F
151	Prkcc	VPSLCGVDHTDRRGRLQLEI	E156D
152	Prrc2b	MMPSYMDPRISPTRTPVDFY	T703S
153	Psd	PSSSLGSGNENDEAGGEEDV	D350N
154	Psg28	MEVSSELFSNVCTSWQRVLL	G11V
156	Rnf26	FTFGGLQALGALLYSCYSGL	T85A
157	Rrs1var4	QFARLKGIRPEKKTNLVWDE	D134E
158	Shank2	KYETDLGKDRKADDKKNMLI	R702K

Supplementary Table 1.1 (continued)

Peptide Identifier	Gene Name	20mer Peptide Sequence	Mutation
159	Slc27a3	QGFLHFHDRTEDTFRWKGEN	G529E
160	Tatdn2	EESHTKVSVEASALDRSS	K286N
161	Thrap3var3	GRGAFPRGRGWFMRKSSTS	R906W
162	Thrap3var2	HDKFSGEEGEMEDDESGTEN	I930M
163	Ttnv2	GVGPLESAPALMKNPVLP	E25599A
164	Usp28	YNDISVTESSLEELERDSYG	W631L
165	Wdfy3var2	TELCHPPRHMAQKEQEEKLY	T43A
166	Wnt3	SCEVKTCWWAEPDFRAIGDF	Q224E
167	Zfp423var2	LAHIHQAHANHHKHKCPMCPE	Q329H
168	Zfp687	LKTHFRTHGMPFIRARQGGS	A1225P
169	Braf	APPSDSTGPQTLTSPSPSKS	I313T
170	9530053A07Rik	RVQAFRHGTDTVIETKFGLL	M938T
171	Abcc6	AFRAQASFTAEDDALMDENQ	Q1144
172	Acsm2	TFHMNIKKLIHQWGHQEAP	P32H
173	Ap2a2	AKTVFEALQAAACHENLVKV	P489A
174	Arfgef1	CAVSMDELLSATHPRMFSLQ	T1155
175	Bsg	MAAALLPLAFTLLSGQ	A8P
176	Ccdc67	KCSQFQKQAQTYQTQLNGKK	N186T
177	Cd63	VKFLLYVLLPFCACAVGLI	A20P
178	Chadl	LEGNMLEELRAGTFGALGSL	P150A
179	Clasp1	ALQSHLKNSDNIVSLPQSDR	S545N
180	Cog8	SRVGADFRGQVAPVFQRVAI	L373V
181	Col17a1	YSNVTQDLMDVFQTYGTIPG	F1366
182	Cpq	AEITGSMYPEQVVLVSGHLD	E281Q
183	Cspg4	EGISVELEVLATVIPLDVQN	P1360
184	Cwc22	AQQRTEKFFALLAGRFCML	G507A
185	Dennd4a	TALSGGRSDLVYNSLSKDNV	G908V
186	Dmbt1	PTDQTTAEQTTVPDYTPIGT	P448T
187	Dnah11	YNYTTPRSFLEQISLFKSL	K3048
188	Dnah5	SDVTWFDKAVGSLVEEEFGE	V2845
189	Dnah6	LYGEVNNVTWKWDGLMALS	E1806
190	Edem3	DIIFDIEDYIVTTEAHLPL	F490V
191	Eftud2	LLRLVCKKFFCEFTGFVDMC	G424C
192	Glrx	IQSGKVVFITPTCPYCRKT	K20T
193	Gm13154	RLSFAQRTLYMDVMLENN	I39M
194	Gm7120	LGIFCLVADRFLRFPIIQHN	L59F
195	Gsg2	NLQHFHRTVLRFSATDLLC	S739R
196	Hebp1	MGMTVPVSAVFPNEDGSLQ	L86V

Supplementary Table 1.1 (continued)

Peptide Identifier	Gene Name	20mer Peptide Sequence	Mutation
197	Hmcn1	VHVSDTGRYVWVAVNVAGMT	C2362
198	Hydin	AVSPAVHFSFSPSHNFGTCFI	T4349
199	Igsf9	AGVVGGVCFLAVAVLVSILA	G747A
200	Il6st	MSAPTIWLAQALLF	R5T
201	Kansl1	ELRAELLGRQAVLEFSLENL	P129A
202	Lrfr1	MTSLVHLTSLNTIGQVAAG	R98L
203	Mcm8	IPHQLLRKYIAYARQYVHPR	G636A
204	Megf11	CKLPESYVEIKSPVHLGSP	M1017
205	Mroh1	QCFNTKVLGIMVETKDPALK	K779M
206	Mtcl1	VEQLQKEKSPLRSGSFLCSR	R1272
207	Mycbp2	IRLDKVVPLKGNVYAVRLR	E1822
208	Myh10	SGAGKTENTKNVIQYLAHVA	K190N
209	Myo7b	DVNADTILHYQQLPKYLRG	H1910
210	Myo7b	KVLKELVPQNVTRLMSSEEW	L1962
211	N4bp2	PSTHPLHNSGFDLPDGDGQ	S222F
212	Ndufs6	MAAALTFRRLTL	V4A
213	Nfat5	VQQHPSTPKRYTVLYISPPP	H63Y
214	Nxf3	HKTLSACEILFGSESIKTM	F309L
215	Pcdhb13	SATDSDSGSNGHITYSLLP	A482G
216	Phkb	IGCLGTSKIYPILGKTVVCY	R559P
217	Plekha7	RLFPQLQTYVAYRPHPPQLR	P841A
218	Pnpla7	LSGWWLLWKRCNPLATKVKV	W1153
219	Ppp2r3a	SHRNSLDTNLISMLFQNLSE	T197I
220	Prkcb	KEPHAVFYAAQIAIGLFFLQ	E449Q
221	Rab11fip5	PVPRPHNSISYTLQSQVLG	S992Y
222	Rimbp3	KEMQGLQFQVHPSETSETT	G685V
223	Sall4	GKVANTNVTLHALRGTKVAV	Q179H
224	Samd9l	IERYFSEVQDLNSFWHSGVV	S1498
225	Scn9a	EFCKLSDFAATLDPPLIAK	A1795
226	Shroom2	KVVNLLLSRLARVENAL	G1372
227	Slco6d1	QSVPTSWNSMRLGLMSTVWR	S593R
228	Sys1	VLNALTALGMLYFIRRGKQ	L81M
229	Tg	TVCDNSSIQVWCLTAERLGV	G1355
230	Tg	KVGTAWKQVYFLGVPYAAP	R2226
231	Tmem30c	ANSIFNDTITISYNLNSSTQ	L169I
232	Tmem44	VPLTSLSHCKALRTMTAISR	P325A
233	Trpv4	TKKCPGVNSLLVDGSFQLLY	F544L
234	Tspan15	IYSTVFWLIGSLVLSVGIYA	G36S

Supplementary Table 1.1 (continued)

Peptide Identifier	Gene Name	20mer Peptide Sequence	Mutation
235	Tspy13	QADGAHLQLVLRFGMRRLH	R151L
236	Ttc3	PAFRTSLNFVQTERGFRKTK	E390Q
237	Ttn	IKIVRLTTGSAYQFRVCAEN	E190I
238	Tubg1	EGFVLCHSIAWGTGSGLGSY	G143W
239	Usp19	VQQRPPQVPSISISKCAACQR	P829S
240	Usp51	DAVVTKATMEQLLNSEGYLL	E642Q
241	Vstm4	NSSGETVTSVPSLAPLPQK	T231P
242	Wdr11	PPLTTKNIKMSQPLLAVGTS	Y483S
243	Zbtb16	DLTKMGMIQLHNPSHPTGLL	Q12H
244	Zfp180	KGRGQVLNHSMLVGGQQELL	V220M
245	Zfp930	ECGKGFAHYSNLRKHGSTHT	T172N

Discussion

Whole-exome sequencing analysis identified 878 non-synonymous single nucleotide substitutions in the Panc02 tumor cell line, which is on par with levels observed in hyper-mutated cancers. It is of interest that although there are several mutations that are predicted to bind strongly to the mouse MHCI molecules, the epitopes that induce the strongest CD8+ T cell responses do not necessarily have the best predictions. In fact, several of the epitopes that induce the most robust T cell responses are classified as weak binders (predicted affinities for MHCI between 50 and 500 nM). This suggests that MHCI binding is a poor indicator of *in vivo* immunogenicity, and that instead there is a threshold for binding that must be reached in order to trigger a T cell response. Specific affinity studies for the reactive epitopes and MHCI molecules are needed to confirm this. The training sets for the predictive algorithms typically reflect viral antigens, which have fully foreign sequences (as opposed to a single point mutation in an otherwise self-peptide), and this may limit the efficacy of predictions for self-peptides. Additionally, the requirements for processing and presentation of self-peptides may be different than the requirements for foreign antigens, and this could influence the accuracy of the predictions.

Of the total 233 epitopes screened for immunogenicity, no dominant epitopes were identified (defined as an epitope that naturally induces spontaneous T cell immunity). This lack of natural immunogenicity may be due to inadequate levels of antigen presentation, possibly due to poor expression levels of the mutated genes or poor MHC-binding affinities, as discussed above. However, some of the neo-epitopes evaluated were expressed at significant levels based on RNAseq data, while others had high predicted MHC-binding affinities, suggesting that expression level and MHC-binding affinities do not wholly account

for the lack of responses. As the epitopes screened were limited by the predicted affinities, it is possible that any dominant neoantigens had predictive values that fell below the cutoff, or do not induce secretion of interferon-gamma, a phenomenon described by (Duan et al., 2014). A comprehensive screen for all mutations present in the Panc02 tumor cell line, incorporating both multiple cytokine analysis, *ex vivo* peptide-dependent culturing, and MHC tetramer analysis would be necessary to formally address this issue. Finally, it is also possible that the T cell repertoire contains a low frequency of T cells capable of recognizing mutant neo-epitopes, or that these T cells are of low-avidity and undergo apoptosis. Anti-CTLA-4 therapy has been shown to broaden the T cell repertoire in melanoma patients (Kvistborg et al., 2014), while anti-OX40 therapy has been shown to improve survival of low-avidity, tumor-reactive T cells (Black et al., 2014), therefore it is reasonable to hypothesize that treatment with CTLA-4 blocking or agonist OX-40 antibodies would uncover T cells reactive to dominant neoantigens. However, the identification of a vaccine-inducible repertoire allows for tumor types which would classically be thought of as poor targets for immunotherapy, either due to their low mutational burden or lack of naturally-occurring tumor rejection antigens, to become candidates for immunotherapy. Although the risk of off-target T cell reactivity exists, it is lower for unenhanced, naturally-occurring T cells, and screening for peptide-induced T cell reactivity to normal tissues can mitigate the risk (Linette et al., 2013).

CHAPTER TWO: OPTIMAL ACTIVATION OF T CELLS FOR EFFECT TUMOR REGRESSION

Summary

The identification of epitopes from the Panc02 tumor line that are capable of inducing CD8⁺ T cell responses reveals that despite a lack of natural immunity, it may still be possible to engage the adaptive immune system to mount an effective antitumor response. Our group has previously shown that T cells reactive to subdominant epitopes are contributors in a vaccine-induced antitumor response to a tolerized breast cancer model (Uram et al., 2011), but this study is the first to show that vaccine-induced T cells reactive to subdominant epitopes can be protective in a pancreatic model of cancer.

The combination therapy employed in this study is designed to both optimally mature APCs so they can effectively activate effector T cells against a multitude of tumor antigens, as well as reprogram the effector T cells for maximal cytolytic activity in the presence of an immunosuppressive environment. Furthermore, we show that this combination may also improve survival by suppressing the activation of inducible Tregs, resulting in less suppression of the vaccine-induced effector T cell population. While more work needs to be done to determine which epitopes are driving the response and determining how the effector T cell compartment is reprogrammed by the addition of agonist OX40 antibodies, the fact remains that these significant antitumor effects on what is considered an aggressive model of PDA indicates that tumor immunotherapy should not be limited to classically immunogenic tumors.

Introduction

Successful tumor immunotherapy requires a T cell repertoire that can be translated into a durable *in vivo* response. Clinical responses to single-agent immune checkpoint therapy are typically seen in tumors with high mutational loads, such as melanoma, lung cancer, and some colorectal cancers (Brahmer et al., 2010; 2012; Topalian et al., 2012; Lipson et al., 2013). Both the neoantigens and altered peptide ligands identified in chapter 1 have been shown to be a part of the inducible repertoire and not naturally primed, either by the tumor or by a whole cell vaccine. Previous studies have shown that the inducible repertoire is a suitable target for immunotherapy (Carreno et al., 2015). Therefore, it is necessary to define a potent, T cell activating vaccine that is capable of stimulating tumor-specific, cytolytic responses, which may require modulation by checkpoint antibodies. The core requirements are suitable antigen targets, which were identified in chapter 1, and potent maturation of antigen-presenting cells. Additional considerations include agents to allow for maintained activation of T cells, regardless of their avidity, as well as modulators to prevent exhaustion within the tumor microenvironment. Ideal adjuvants allow for high levels of sustained presentation of antigens, as well as expression of costimulatory molecules and cytokines to fully activate significant numbers of antigen-specific T cells. This can be achieved by stimulating APCs through Toll-like receptors (TLR), innate immune receptors, and compounds that activate the stimulator of interferon genes (STING) pathway. Although other adjuvants were tested, two adjuvants were primarily used throughout the course of these studies: polyinosine-polycytidylic acid (poly I:C), a TLR3 agonist, and R243, a human STING-activating cyclic dinucleotide adjuvant.

The immune checkpoint molecule programmed death receptor-1 (PD-1) and its ligand, programmed death ligand-1 (PD-L1), serve as major immune tolerance mechanisms that can attenuate antitumor cytotoxic T cell responses (Flies, Chen, 2007). PD-L1 can be found on tumor cells as well as intratumoral APCs, and its expression in the tumor microenvironment (TME) has been shown to correlate with poor prognosis in patients with epithelial neoplasms, including PDA (Ohigashi et al., 2005; Thompson et al., 2006; Wu et al., 2006; Nomi et al., 2007; Zou, Chen, 2008). Antibodies that block the interaction of PD-1 with PD-L1 have shown clinical activity in a variety of human malignancies, including melanoma, NSCLC, renal cell, bladder, gastric and colorectal cancers (Brahmer et al., 2010; 2012; Topalian et al., 2012; Lipson et al., 2013; Le et al., 2015), and two anti-PD-1 antibodies are already FDA approved for the treatment of melanoma (Nivolumab and Pembrolizumab) and NSCLC (Nivolumab). The clinical activity of antibodies that block the PD-1/PD-L1 T cell signaling pathway is associated with higher pre-treatment levels of tumor-infiltrating CD8⁺ effector T cells and higher PD-L1 expression in the TME, suggesting that blockade of this signaling pathway works by boosting naturally occurring cancer associated T cells that are suppressed by PD-1 signaling within the TME. Furthermore, these findings suggest that patients whose tumors are not naturally infiltrated with effector T cells and/or whose tumors lack PD-L1 expression are poor candidates for PD-1/PD-L1 signaling blockade.

Emerging data suggest that the T cells that are most susceptible to activation by PD-1 blocking antibodies leading to tumor rejection and control are T cells that recognize mutant neo-epitopes (Topalian et al., 2012; van Rooij et al., 2013; Snyder et al., 2014; Rizvi et al., 2015; Van Allen et al., 2015; Hugo et al., 2016). For example, clinical responses to PD-1

blockade have been observed primarily in tumor types associated with high mutation burdens which have a higher likelihood of generating mutant neo-epitopes. In addition, patients with NSCLC and melanoma who have high mutational loads in their tumors are most often the patients who demonstrate clinical responses to PD-1/PD-L1 blockade. Altogether, these data indicate that neo-epitopes capable of triggering spontaneous T cell responses are uncommon, which may explain why the majority of patients with all cancer types do not respond to PD-1/PD-L1 blockade as a single agent therapy. However, whether tumors that do not respond to PD-1/PD-L1 blockade completely lack neo-epitopes capable of being recognized by the immune system has so far not been addressed.

Several studies have shown that costimulation of the OX40 pathway results in expansion, prolonged survival, and enhanced effector function of CD8⁺ T cells through the NF- κ B pathway, while the effects on regulatory T cells can result in expansion, deactivation, or apoptosis and is decided by the local milieu (Colombo, Piconese, 2007; Vu et al., 2007; Hirschhorn-Cymerman et al., 2009; Ruby et al., 2009). Treatment with agonist anti-OX40 antibodies can augment the endogenous T cell response as well as enhance T cell priming by vaccines. In a murine model of breast cancer, the addition of OX40 to an autologous whole cell vaccine was able to break tolerance to the *neu* tumor antigen, and resulted in improved antitumor immunity (Murata et al., 2006). In addition to its role in T cell proliferation, OX40 has also been shown to increase survival in low-avidity T cells. Low avidity T cells present a challenge for tumor immunotherapy on two fronts: they are subject to deletion in the presence of continuous, small amounts of antigen, a common occurrence in tumor development, and they can induce apoptosis of high avidity tumor-reactive T cells (Black et al., 2014). This is of particular importance in this vaccine model, which is comprised of

multiple subdominant epitopes that induce T cells of unknown avidity. It has also been found that anti-PD1 and anti-OX40 can act synergistically, as shown by the induction of mesothelin responses in a mouse model of ovarian cancer (Guo et al., 2014).

PDA, the fourth leading cause of cancer deaths in the United States (Siegel et al., 2016), is an example of a tumor type that does not respond to PD-1/PD-L1 blockade as a single agent therapy (Brahmer et al., 2012). Likewise, PDA is not naturally infiltrated with high numbers of effector T cells, and is not considered a hypermutated cancer type, typically accumulating as few as 45 somatic mutations (Jones et al., 2008; Vogelstein et al., 2013). Here we use the PD-1/PD-L1 blockade-resistant Panc02 murine cell line as a model of PDA, to demonstrate that vaccination can induce novel T cell responses against subdominant neo-epitopes that are not spontaneously primed by the tumor, resulting in increased CD8⁺ T cell accumulation and upregulation of PD-1 and PD-L1 expression in the TME, which then sensitizes the tumor to treatment with PD-1 blocking antibodies. These data suggest that the neo-epitope landscape that can be targeted with vaccines is larger than would be predicted by examining spontaneous neo-epitope-specific T cell responses in tumor-infiltrating lymphocytes. Thus, immunization against mutant neo-epitopes provides a potential strategy for converting immune checkpoint blockade-resistant tumors into immune responsive tumors.

Results

Comparison of adjuvant choice

A vaccine-inducible T cell repertoire that has an anti-tumor effect requires potent T cell activation with maintained functionality within the immunosuppressive tumor microenvironment. For an optimal anti-tumor effect, it is necessary to induce a strong CD8⁺ effector T cell response. We tested several adjuvants that have been shown to elicit robust, vaccine-specific CD8⁺ responses with peptides in clinical trials, in order to facilitate translation of our vaccine to a clinical setting. Polyinosine-polycytidylic acid (poly I:C) is a double-stranded RNA synthetic analog that has shown potent activity as a TLR3 agonist. Stimulation of TLR3 by poly I:C results in type I interferon production and IL-12 cytokine production, thereby promoting the generation of Th1/CD8⁺ cellular immunity (Salem et al., 2005; Celis, 2007; Currie et al., 2008; Pulko et al., 2009). R243 and R287 are human STING-activating cyclic dinucleotide (CDN) agonists developed by Aduro biotechnologies. STING agonists have shown potent antitumor activity by inducing type I interferon production and maturation of BATF3-lineage dendritic cells, resulting in recruitment and activation of effector T cells. AddaVax is a squalene-based oil-in-water emulsion that has been shown to elicit both Th1 and Th2 immune responses and was used in combination with poly I:C and the STING reagents (Ott et al., 1995; 2000; Calabro et al., 2013). Montanide ISA51 and Montanide ISA720 are both developed by Seppic and have been used in clinical trials. ISA51 generally induces more of a Th1/CD8⁺ T cell response, while ISA720 generally induces a Th2/CD4⁺ T cell response (Aucouturier et al., 2001; 2002; Ascarateil et al., 2015). Animals were immunized according the schedule in **Figure 1.1B** and as described in methods, and then CD8⁺ T cell responses were measured by ELISpot as described in methods, results are

shown in **Figure 2.1**. Flow cytometry analysis of vaccine-induced CD8⁺ T cells was used in an effort to measure the polyfunctionality of the vaccine-reactive T cells induced by R243 in combination with AddaVax. CD8⁺ T cells were stimulated with T2 APCs overnight in the presence of protein transport inhibitors and the 2 peptides inducing the strongest response, with Ova included as a negative control. More than 10% of the isolated CD8⁺ T cells expressed interferon-gamma and PD-1 (a marker of activation) when stimulated with the Panc02 peptides #44 (corresponding to protein Glb1l2:pG36C) or #237 (corresponding to protein Ttn:p.E19018A), with the majority of these also expressing TNF α and Granzyme B (**Figure 2.2**). Based on these results, we opted to use poly I:C in combination with AddaVax and R243 in combination with AddaVax to test whether immunization with a Panc02-specific peptide vaccine would result in clearance of tumor lesions. The structure of R243 is shown in **Figure 2.3**.

Antitumor efficacy of both adjuvants

After determining that immunization with R243 in combination with AddaVax and poly I:C in combination with AddaVax induced the most robust CD8⁺ T cell responses in tumor-naïve animals, as measured by interferon-gamma, we next sought to determine whether this translated into an effective antitumor response. Mice were challenged with Panc02 cells and 3 days later, after tumors had established, were treated with the Panc02-specific peptides listed in **Table 2.1**. A boosting vaccine dose was given on day 10 post-tumor challenge and tumor growth was monitored every 3-4 days until tumors reached 10x10 mm², at which point mice were euthanized. Time to measurable tumor development (shown as a Kaplan-Meier curve) and tumor measurements are shown in **Figure 2.4**. All vaccine

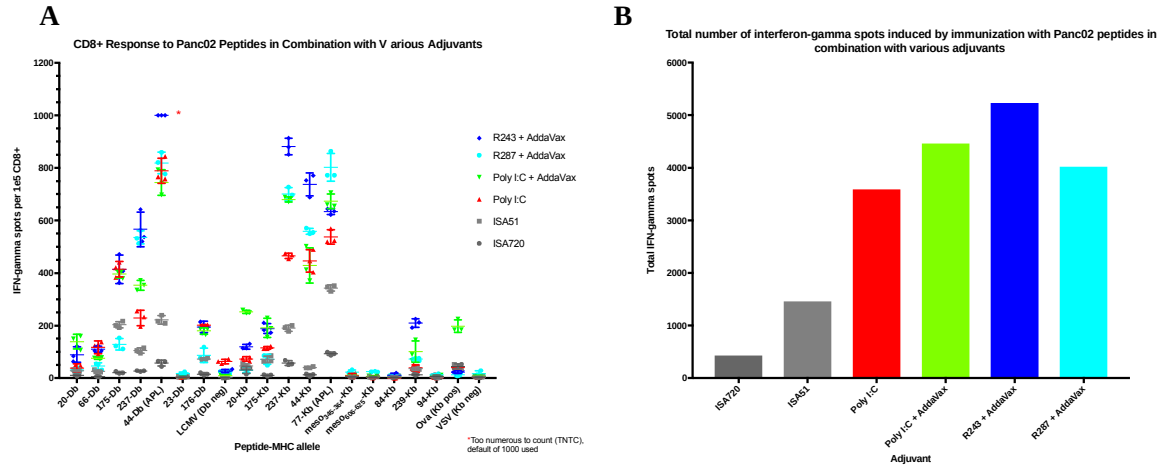


Figure 2.1 Induction of interferon-gamma in CD8+ T cells stimulated with Panc02 peptides

(A) Mice were immunized with pooled 20mer peptides corresponding to the mutant neoepitopes and altered peptide ligands, and isolated CD8+ T cells were analyzed for interferon-gamma production as described in methods. Wells that were saturated were marked as “too numerous to count (TNTC)” and a default value of 1000 spots was used for analysis. Altered peptide ligands are marked as “(APL)” after the peptide identifier and MHC-restricted allele. Symbols represent each replicate with a line at the mean \pm SEM.

(B) The total number of interferon-gamma spots induced by all peptides in **(A)** was summed and graphed to get a measure of the total induced repertoire.

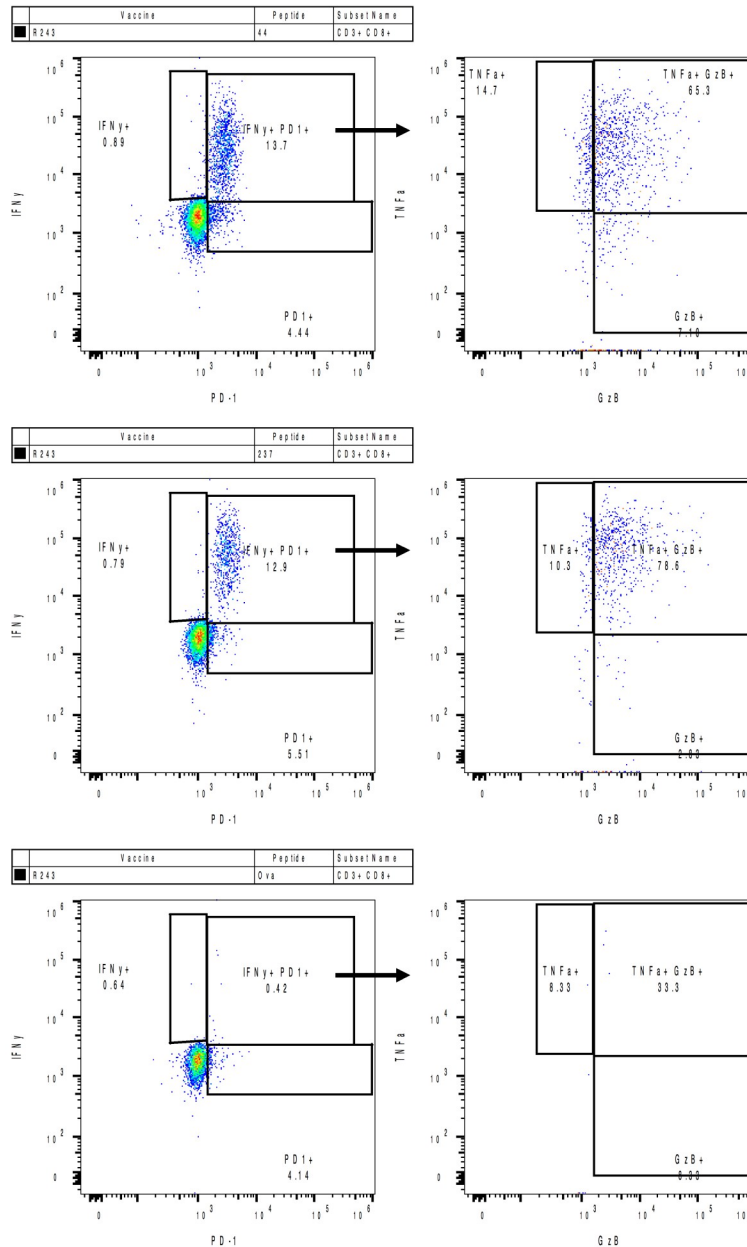


Figure 2.2 Panc02 peptides immunized with R243 and Addavax induces polyfunctional CD8+ T cells

Overnight stimulation with Panc02 peptides presented by T2 APCs induces a robust, polyfunctional CD8+ T cell response by flow cytometric analysis. Live, CD3+ CD8+ T cells were gated and then graphed for IFN γ and PD-1 expression. Granzyme B by TNF α graph shows cells gated on both IFN γ and PD-1 as denoted by arrows.

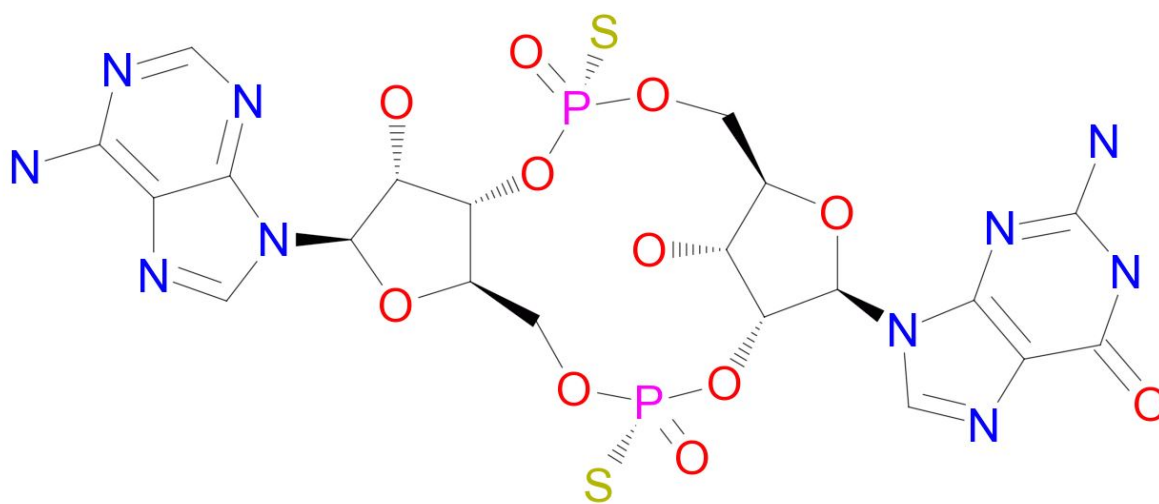


Figure 2.3 Structure of the R243 STING agonist

Courtesy of Aduro Biotech

Table 2.1 Immunogenic Panc02 peptides used to test for antitumor efficacy

Peptide Identifier	Protein	Mutation	Predicted Affinity (nM)
20	Myo1g	K696N	24
23	Ace	G473A	23
44	Glb1l2	G36C	327
66	Map2k5	A11G	343
77	Rasa3	T203S	155
84	Clcn7	D771G	256
94	Notch2	A1969S	49875
175	Bsg	A8P	425
176	Ccdc67	N186T	857
237	Ttn	E19018A	31
239	Usp19	p829S	862
Meso3	Mesothelin 345-364	none	5540
Meso6	Mesothelin 606-625	none	508

Full peptide sequences can be found in **supplemental table 1.1**.

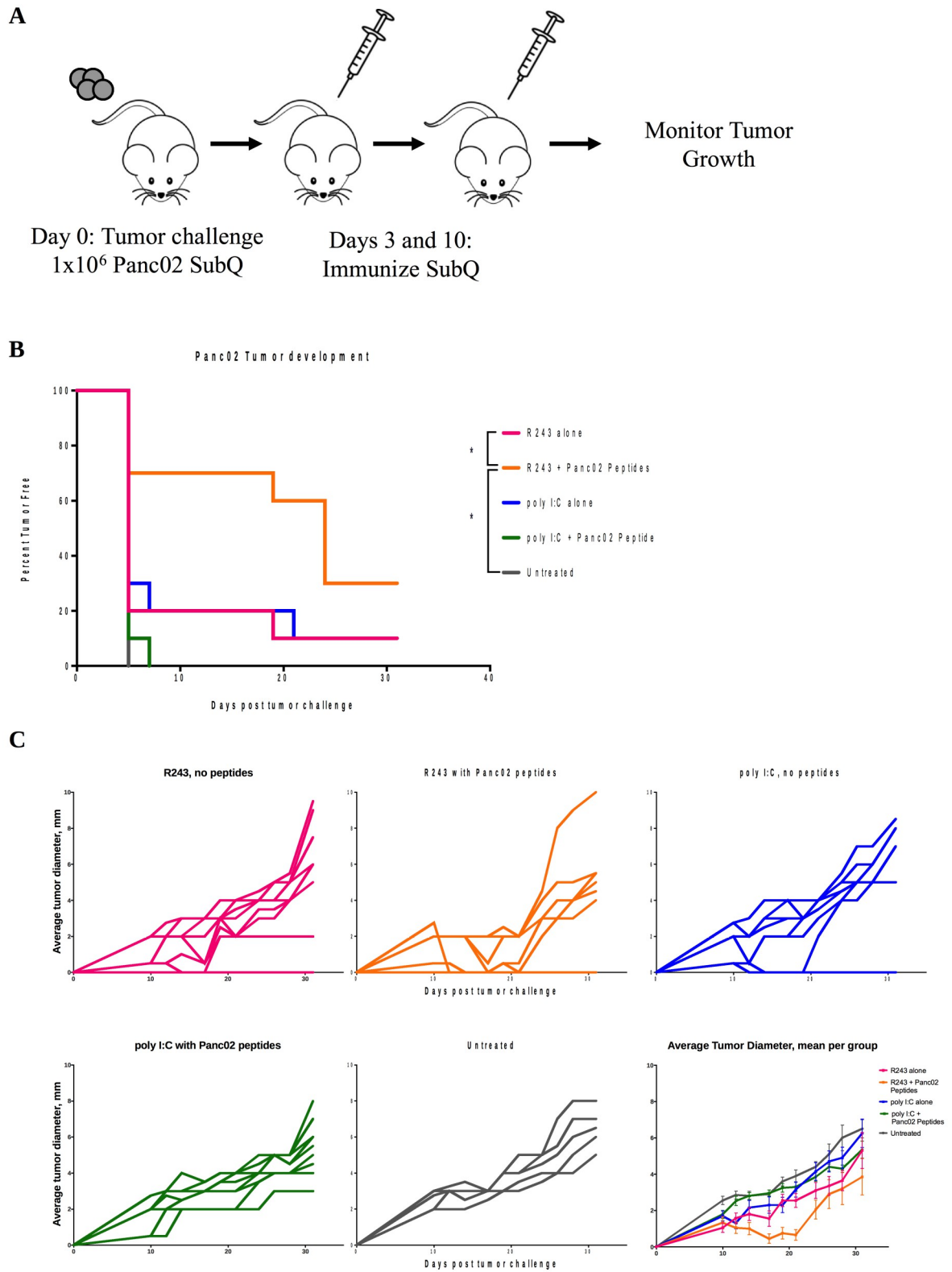


Figure 2.4 Immunization with R243 and Panc02peptides provides a survival benefit

(A) Treatment scheme. Mice were tumor challenged subcutaneously in the rear limb as described in methods on Day 0. On Days 3 and 10, mice were immunized with the described vaccine mixtures subcutaneously, once on either side of the base of the tail. Tumor growth was measured with calipers and monitored until tumors reached 10x10 mm.

(B) Kaplan-Meier Curve showing time to tumor development of tumor-challenged, immunized mice, 10 mice per group. *P < 0.03 by log-rank (Mantel-Cox) test

(C) Spider plot of individual mouse tumor measurements, plotted as average tumor diameter (mm), with the mean tumor diameter \pm SEM shown in the 6th panel.

compositions included AddaVax. While there was a survival benefit when mice were immunized with the Panc02-specific peptide vaccine in combination with the R243 adjuvant, tumors eventually developed in many of the treated animals. To prove that T cells are mediating the anti-tumor effect, T cell depletion experiments are on-going.

Checkpoint potentiation of Panc02 vaccine

As the Panc02 peptides demonstrated a survival benefit but not complete tumor rejection when given as a vaccine composed of AddaVax and R243, we hypothesized that T cell exhaustion had occurred and was responsible for the eventual tumor recurrence. When tumor bearing mice are treated with Panc02-specific peptides using R243 as an adjuvant, CD8⁺ T cells that have infiltrated the tumor microenvironment express the exhaustion markers PD-1, Lag3, and Tim3 on their surface (**Figure 2.5**). Furthermore, PD-L1 expression on Panc02 tumor cells has been seen both with *in vitro* stimulation using interferon-gamma as detected by flow cytometry (**Figure 2.6**), and *in vivo* with the metastatic hemispleen model when mice are treated with a GM-CSF secreting autologous vaccine, but not in untreated, tumor-bearing animals (Soares et al., 2015). While one group reported that in a murine model of PDA, PD-L1 upregulation was primarily seen on infiltrating immunosuppressive cells and not tumor cells in response to T cell derived interferon-gamma (Winograd et al., 2015), these differences may be the result of differences in tumor implantation (subcutaneous versus metastatic models) and would exert similar immunosuppressive effects on the T cells. Therefore, we attempted to improve tumor clearance rates by modulation of two checkpoint molecules. Anti-PD-1 antibody therapy has

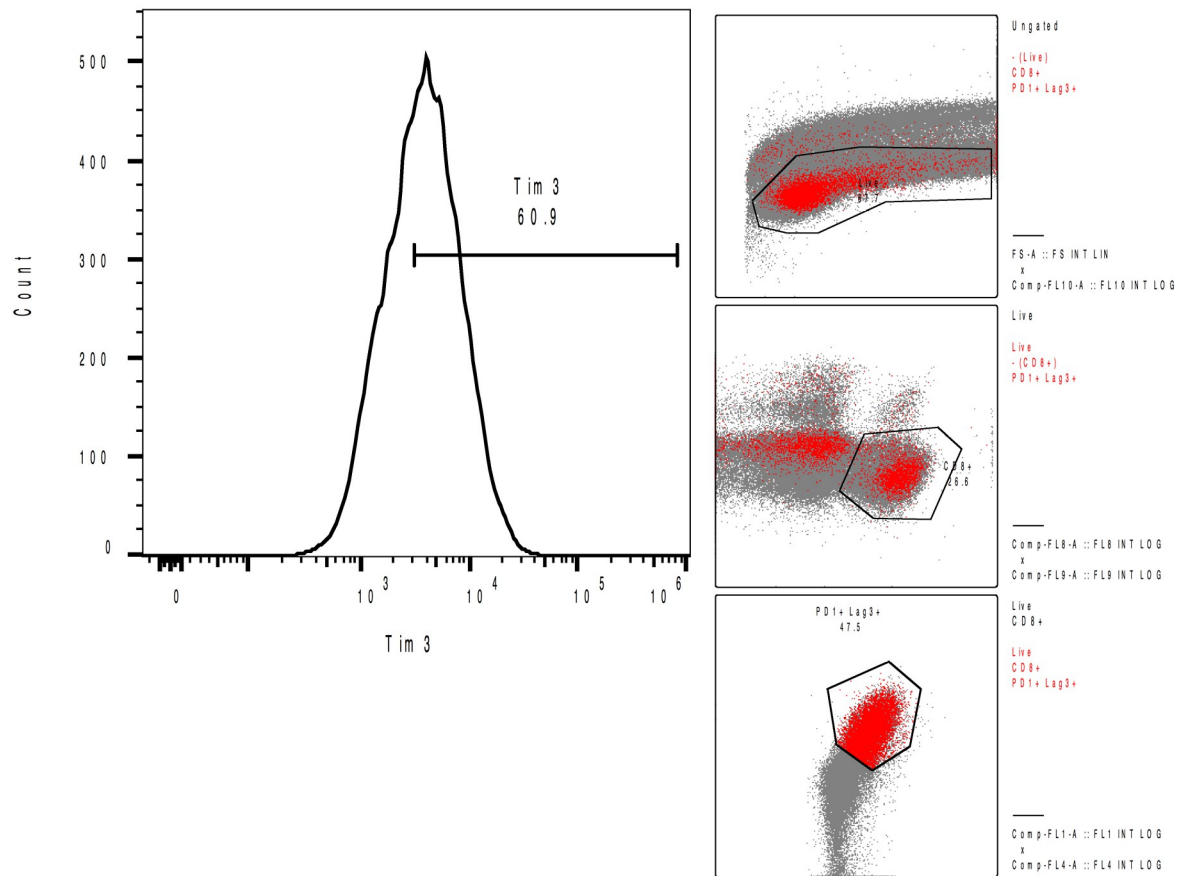


Figure 2.5 Expression of exhaustion markers on tumor-infiltrating T cells

Flow cytometry analysis of cell surface exhaustion markers of tumor infiltrating lymphocytes from mice treated with Panc02 peptides and R243. One sample shown that is representative of typical staining results. Backgate analysis is shown in the right side graphs. Cells were gated on Live, CD8+, PD-1+ and Lag3+.

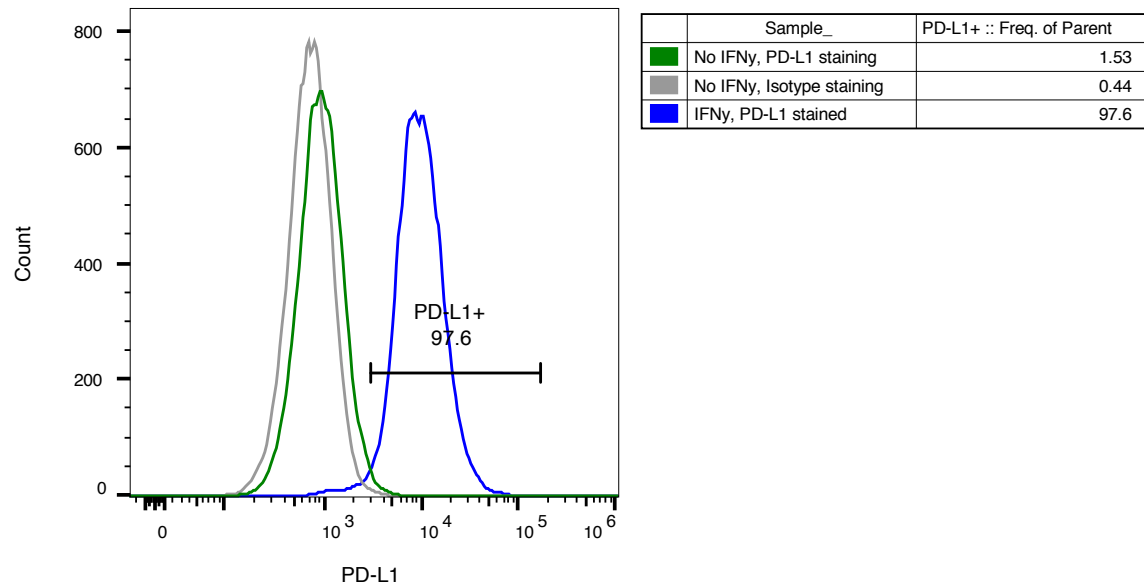


Figure 2.6 *In vitro* stimulation of Panc02 tumor cells by IFN γ results in surface PD-L1 expression

Panc02 cells were cultured in the presence or absence of 10 ng/mL mouse IFN γ for 72 hours as marked. Cells were then stained with anti-mouse PD-L1 or control isotype antibody and analyzed by flow cytometry.

previously been shown to augment vaccine efficacy in several tumor models, including the metastatic Panc02 hemispleen model. We included an agonist anti-OX40 antibody at days 1, 3, and 7 post-vaccine to determine whether we could detect CD8⁺ T cell responses to some of the Panc02 peptides that induce low or no interferon-gamma when used in immunization. We hypothesized that the inclusion of the agonist anti-OX40 antibody would increase the formation of the vaccine-specific memory T cell compartment, culminating in a durable anti-tumor response. As it has been shown that low-dose cyclophosphamide (Cy) in combination with the anti-CD25 depleting antibody PC61 depletes regulatory T cells (Treg) (Emens, 2005), we included this as a treatment condition to determine if Treg cells were exerting an inhibitory effect on effector T cells that were infiltrating the tumor microenvironment. Finally, we slightly modified the peptide vaccine to include 2 of the putative CD4⁺ T cell epitopes and exchanged one of the peptides that induced a weak interferon-gamma response for one that induced a more robust interferon-gamma response. The full list of peptides included in the Panc02-peptide R243 vaccine (STINGVac) is in **Table 2.2**.

Mice were tumor challenged with Panc02 cells in the hind limb as before, but tumors were allowed to develop until they were palpable before treatment was begun. Once tumors were palpable (between 1 and 3 mm²), mice were dosed according to the timeline in **Figure 2.7A** and tumor growth was monitored every 3-4 days. As shown in **Figure 2.7B-D**, Panc02-specific peptide STING vaccination modulated with both anti-OX40 and anti-PD-1 demonstrated near-complete tumor eradication, whereas single checkpoint blockade gave a modest survival benefit compared to vaccine alone. Interestingly, the addition of the Treg depleting conditions resulted in a delayed anti-tumor effect, however the

Table 2.2 Panc02 peptides used in R243 vaccine (STINGVac) checkpoint-blockade

Peptide Identifier	Protein	Mutation	Predicted Affinity (nM)	Experimental Allele Restriction	WT Cross-reactivity	Neoepitope or Altered Peptide Ligand (APL)
20	Myo1g	K696N	24	Kb, Db	ND	Neo
23	Ace	G473A	23	Db	ND	Neo
44	Glb1l2	G36C	327	Kb, Db	Yes	APL
66	Map2k5	A11G	343	Db	Yes	Neo
77	Rasa3	T203S	155	Kb	Yes	APL
84	Clcn7	D771G	256	Kb	ND	Neo
94	Notch2	A1969S	49875	Kb	ND	APL
175	Bsg	A8P	425	Kb, Db	No	Neo
237	Ttn	E19018A	31	Kb, Db	No	Neo
219	Ppp2r3a	T197I	2	Kb, Db	ND	Neo
218	Pnpla7	W1153C	435 (H-2-Kb), 2293 (H-2-IAb)		No	Neo
230	Tg	R2226L	12 (H-2-Kb), 1022.9 (H-2-IAb)		No	Neo

Bold are peptides with predicted strong affinity

Red are peptides with strong T cell reactivity

ND: not done

Full peptide sequences can be found in **supplementary table 1.1**.

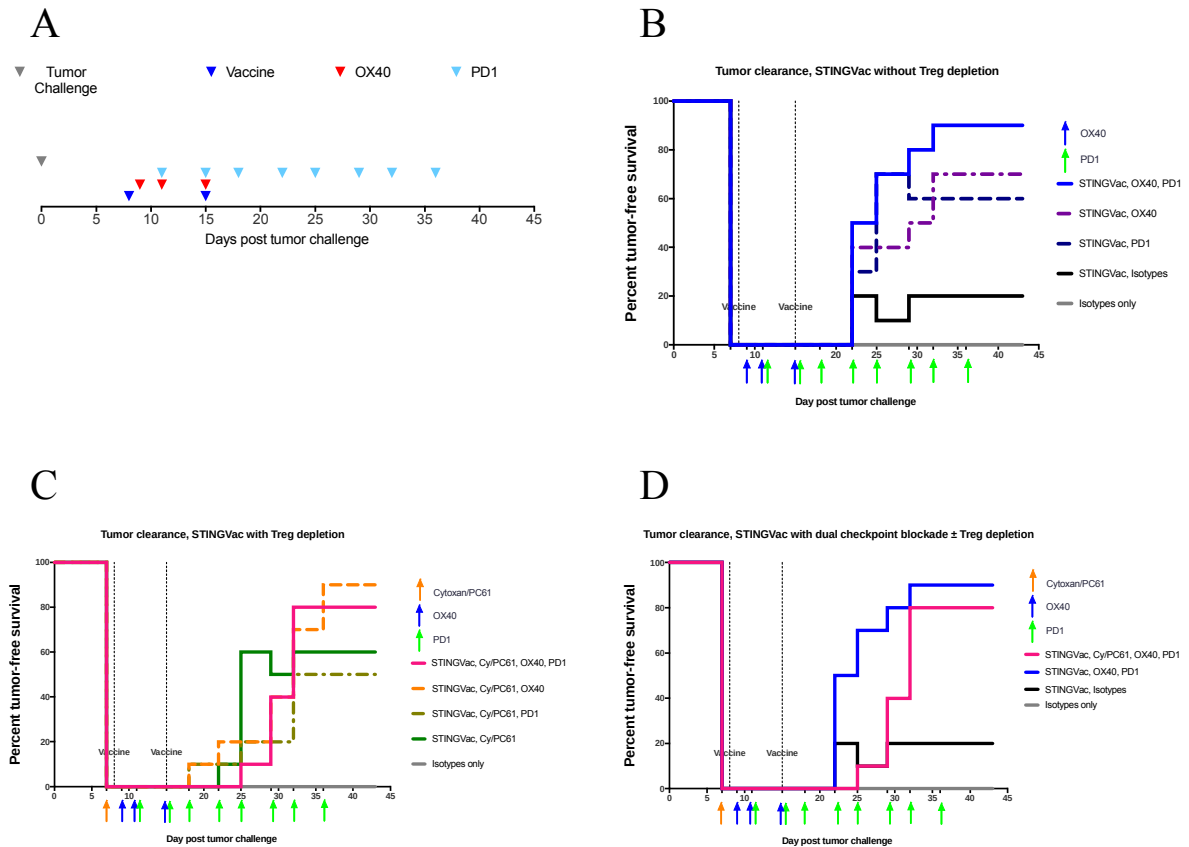


Figure 2.8 STING vaccine in combination with dual checkpoint therapy results in near-complete tumor protection

(A) Treatment schedule. Mice were challenged as in **Figure 2.4A**, and once palpable tumors had developed (around day 7) therapy was initiated as marked. The Treg depletion treatment condition is not shown (low dose cyclophosphamide and PC61, Cy/PC61) was given as a single dose once tumors were palpable and one day prior to vaccine.

(B-D) Tumor clearance rates as a function of time for STINGVac ± checkpoint blockade or isotype control antibodies without Treg depletion **(B)**, STINGVac ± checkpoint blockade or isotype control antibodies with Treg depletion **(C)**, STINGVac + anti-OX40 and anti-PD1 ± Treg depletion condition **(D)**. Isotype only group was treated with isotype control antibodies for checkpoint blockade antibodies without STINGVac as a treatment control group.

combination of Treg depletion, vaccine, and anti-OX40 either with or without anti-PD-1 resulted in near-complete tumor rejection despite the delayed effect (**Figure 2.8D**). Tumor measurements for STINGVac \pm checkpoint blockade without Treg depletion conditions are shown in **Figure 2.9**.

When tumor-infiltrating lymphocytes were analyzed by flow-cytometry from the vaccine and anti-OX40 treated group compared to the vaccine and anti-PD-1 treated group on day 43 post-tumor challenge, there were stark differences in the amount of cytokine and PD-1 expression on the surface of the CD3⁺CD8⁺ T cell populations. While there weren't consistent differences in the number of T cells infiltrating into the tumor microenvironment (**Figure 2.10A**), the CD8⁺ T cells isolated from the mice treated with Panc02 peptide STING vaccine in combination with anti-OX40 had robust interferon-gamma expression with little PD-1 expression, while mice treated with the same vaccine in combination with anti-PD-1 showed diminished interferon-gamma expression and increased surface PD-1 expression (**Figure 2.10B**). Moreover, in the STING-vaccine anti-OX40 treated mice, there was a decrease in the percentage of CD3⁺CD4⁺FoxP3⁺ T cells, classical Treg markers, and an increase in the percentage of interferon-gamma expressing CD3⁺CD4⁺ T cells, indicating that the inducible Treg compartment is being skewed towards an effector phenotype (**Figure 2.10C**). Furthermore, when tumor-infiltrating T cells from these animals are analyzed for exhaustion markers, the STING-vaccine anti-PD-1 treatment group shows an increase in the frequency of CD8⁺PD-1⁺Lag3⁺ cells, while the corresponding anti-OX40 treatment group exhibits almost no expression of these exhaustion markers on the surface of their tumor-infiltrating CD8⁺ T cells (**Figure 2.11**).

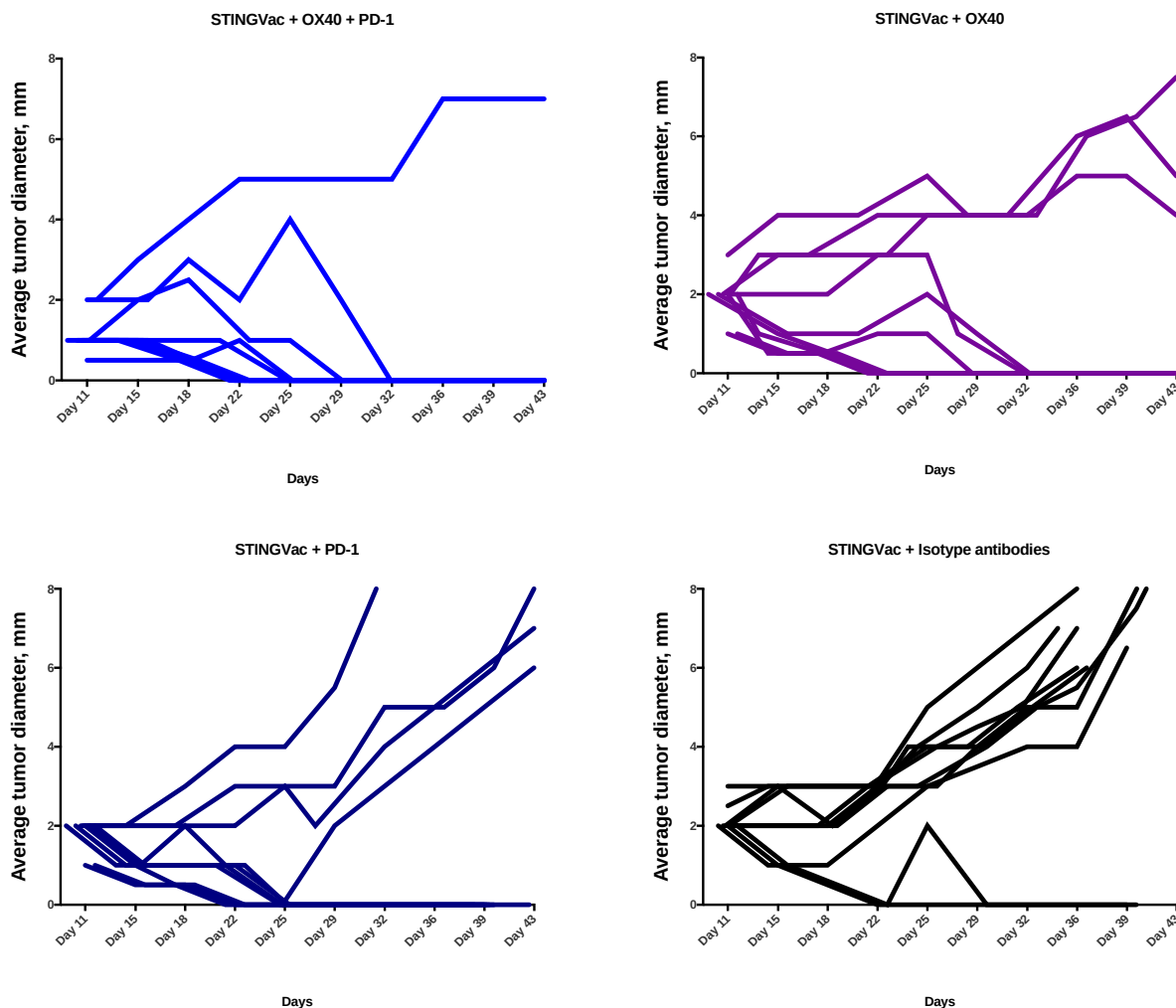


Figure 2.9 Average tumor diameter (mm) in STINGVac-treated mice with or without checkpoint blockade antibodies

Tumors were measured by calipers every 3-4 days starting on day 11.

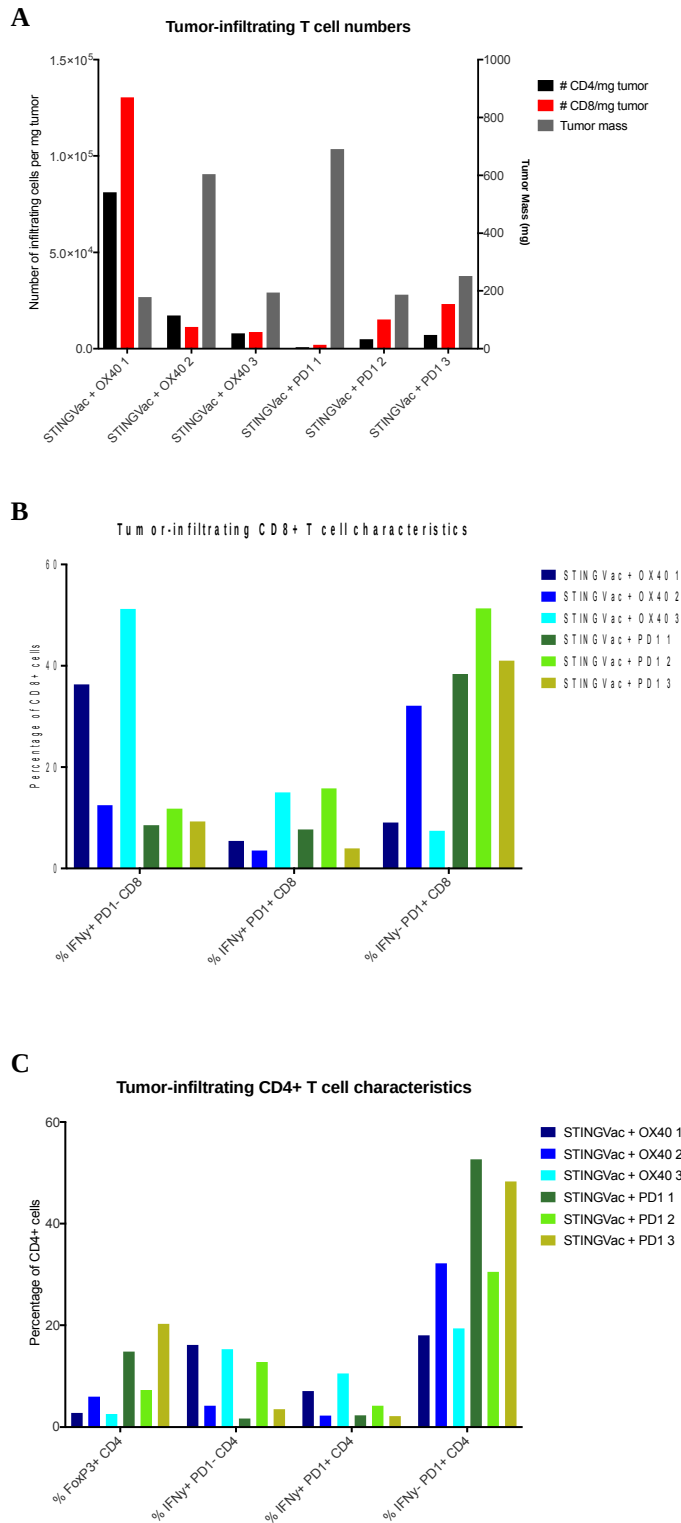


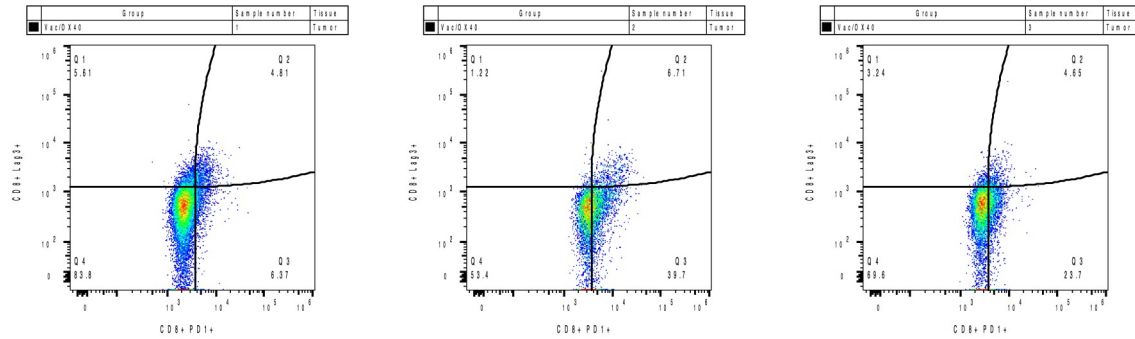
Figure 2.10 Anti-OX40 augments STINGVac-primed T cells to maintain effector function in the tumor microenvironment

(A) The number of tumor-infiltrating CD4⁺ and CD8⁺ T cells plotted on the left Y-axis, with the total tumor weight plotted on the X-axis. Each plotted group represent 1 mouse.

(B) Percentage of CD8⁺ T cells expressing IFN γ , IFN γ with PD-1, or PD-1 alone. Each bar represents cells isolated from a single tumor.

(C) Percentage of CD4⁺ T cells expressing FoxP3, IFN γ , IFN γ with PD-1, or PD-1 alone. Each bar represents cells isolated from a single tumor.

STINGVac + OX40



STINGVac + PD1

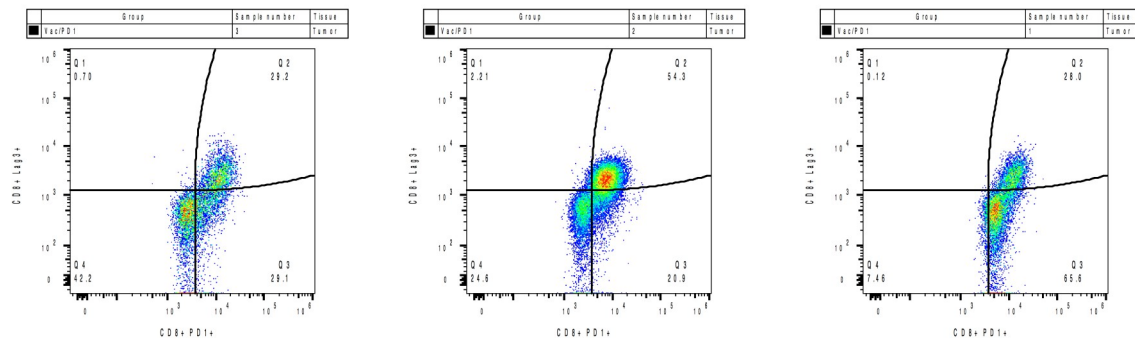


Figure 2.11 Anti-OX40 prevents the expression of exhaustion markers on tumor-infiltrating CD8+ T cells

Immediately after tumor-infiltrating cells were harvested, they were stained for surface expression of exhaustion markers. Sample number are from the same samples in **Figure 2.10**. Cells were gated by size for lymphocytes, then gated for live CD8+ cells.

To demonstrate the durability of the vaccine-induced anti-tumor response, 5 mice per group from STING-vaccine with anti-PD-1, anti-OX40, or anti-PD-1 and anti-OX40 treatment groups that had cleared initial tumor challenge were rechallenged with Panc02 tumors on the contralateral hind limb on day 56 after the initial tumor challenge, 41 days after the last vaccine and anti-OX40 dose and 19 days after the last anti-PD-1 dose. No further therapy was administered and tumor growth was monitored every 3-4 days. Consistent with the initial tumor-rejection results, animals from the STING-vaccine and combination checkpoint blockade demonstrated near-complete eradication, with 4 of the 5 mice rejecting their tumors. STING-vaccine with anti-OX40 resulted in 3 of 5 mice rejecting tumors, while all mice from the STING-vaccine with anti-PD-1 succumbed to the rechallenge (**Figure 2.12**). All mice from the STING-vaccine and combination checkpoint blockade were sacrificed and splenocytes harvested to test for Panc02-peptide specificities (**Figure 2.13**). In addition, tumor was harvested and tumor-infiltrating lymphocytes were harvested and tested for general cytokine and CD4+FoxP3 expression from the one mouse that failed to reject the tumor rechallenge (**Figure 2.14**).

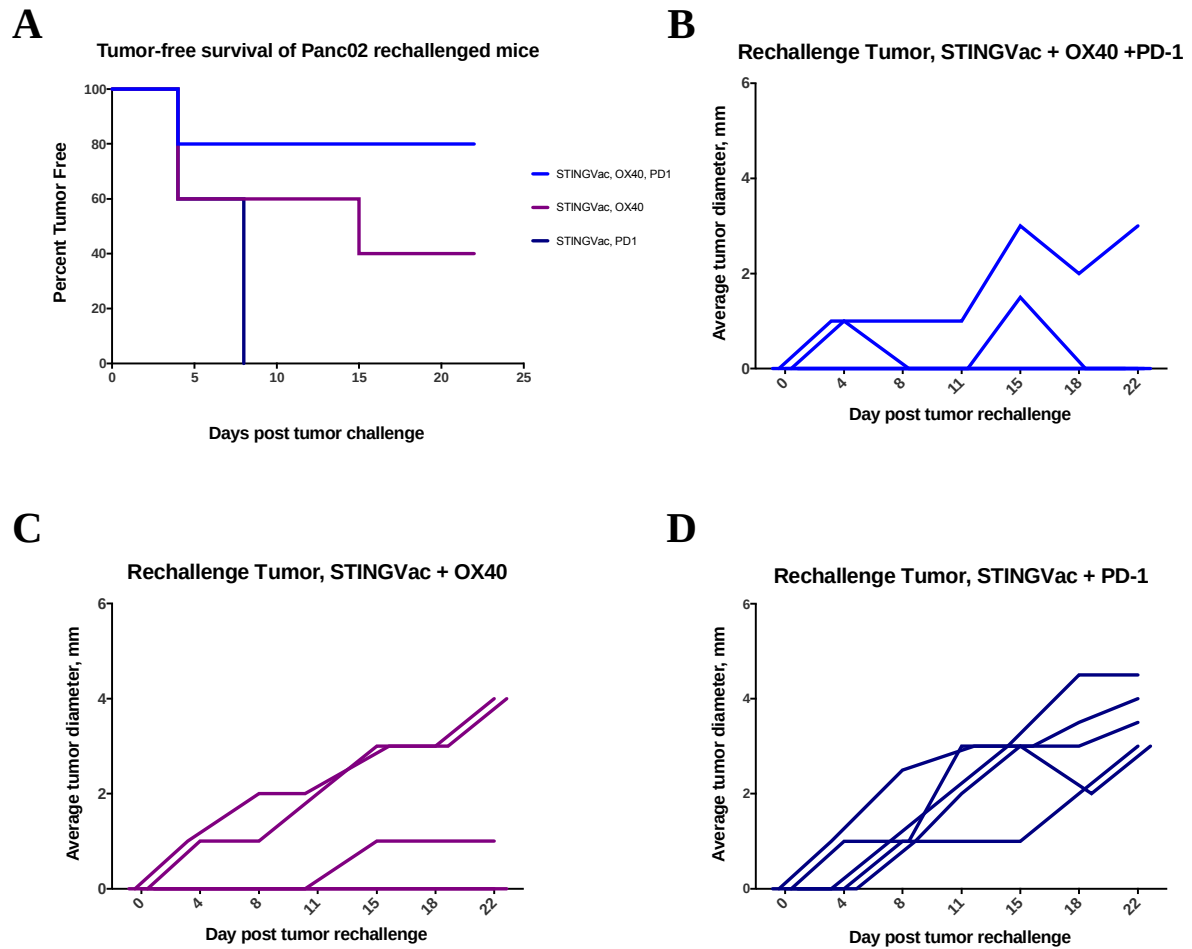


Figure 2.12 Anti-OX40 and anti-PD-1 synergize with STINGVac to provide a durable anti-tumor response

(A) Tumor-free survival of mice rechallenged with Panc02 without additional treatment (n=5 per group).

(B-D) Tumor diameter as a function of time from the groups in **(A)**.

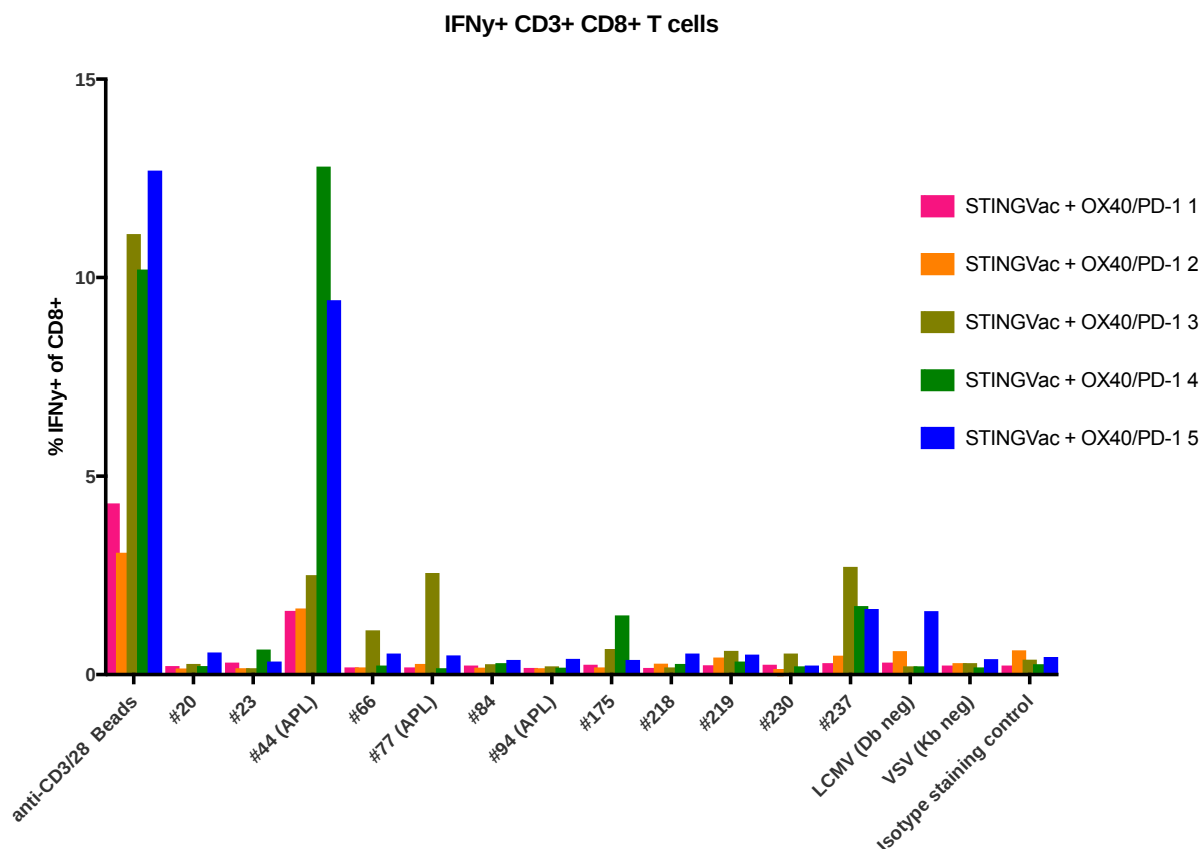


Figure 2.13 Specificities of Panc02-reactive T cells from STINGVac, anti-OX40, anti-PD-1 treated mice

Splenocytes were harvested from each mouse, plated at 2×10^6 cells in 1 mL CTL media with each peptide (2 $\mu\text{g/mL}$) or anti-CD3/28 magnetic beads in the presence of protein transport inhibitors overnight. The following day, cells were washed and stained for intracellular cytokine staining to determine peptide specificities. Each number represents a single mouse, mouse 1 did not eradicate the rechallenge tumor.

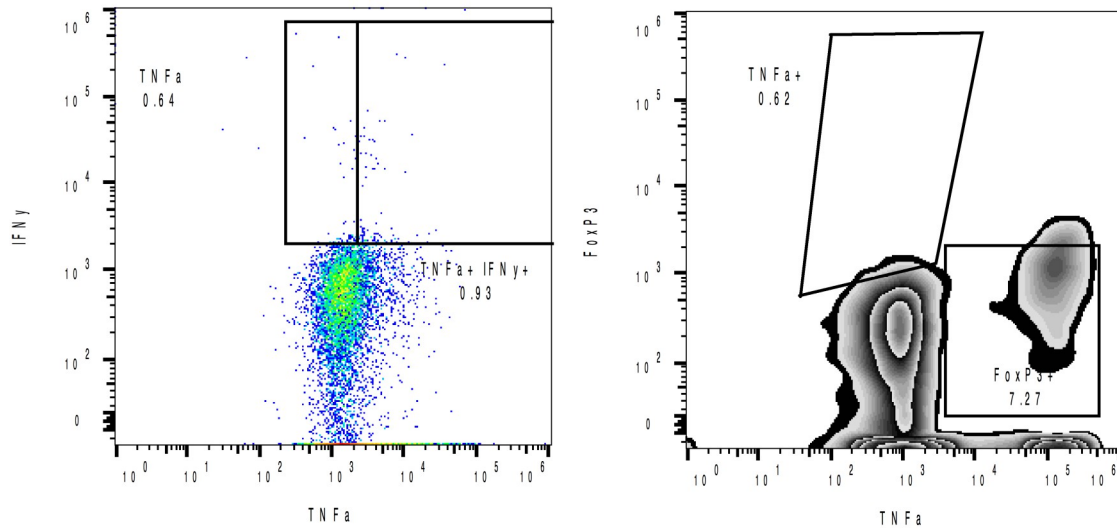


Figure 2.14 Tumor-infiltrating lymphocytes do not express cytokine with anti-CD3/28 stimulation

Tumor-infiltrating lymphocytes were harvested as described in methods and stimulated overnight with anti-CD3/28 magnetic beads in the presence of transport inhibitors. The following day, cells were washed and stained for intracellular cytokine staining to determine peptide specificities. Left side, gated Live CD3+ CD8+ T cells. Right side, gated Live CD3+ CD4+ T cells, contour levels set at 5%.

Discussion

Tumors that contain antigens capable of spontaneously inducing tumor-specific T cells are typically considered ideal candidates for immunotherapy and, in some instances, respond to single-agent immunotherapy, such as treatment with anti-PD-1 antibodies. The lack of efficacy in PDA and other non-responding tumors may be due to a lack of naturally-occurring anti-tumor T cells. A study in three melanoma patients showed that novel T cell responses against mutant neo-epitopes can be induced by immunization, demonstrating that a measurable, pre-existing T cell response is not a requirement for induction of immunity against mutant neo-epitopes (Carreno et al., 2015). We show that tumors for which no dominant mutation is known may still be candidates for combination immunotherapy with the right combination of T cell-activating compounds, without the need for a cell-based vaccine. A vaccine targeting these subdominant epitopes can lead to a durable, protective anti-tumor response that is dependent on a robust, tumor-specific T cell compartment. This effect is not limited to neo-antigens; T cells reactive to shared antigens are important contributors to the anti-tumor effect. Several studies show that direct stimulation of the STING pathway by synthetic CDNs robustly induces tumor-specific effector T cells. Both intratumoral injections of synthetic cyclic dinucleotides targeting the STING pathway and vaccination with whole cell vaccines in combination with synthetic CDNs have shown efficacy in inducing a tumor-specific T cell response, where the tumor itself becomes the source of antigen (Fu et al., 2015; Baird et al., 2016; Moore et al., 2016); however, there is limited data on the efficacy of a tumor-specific peptide vaccine targeting the STING pathway.

It is interesting that despite being well infiltrated with polyfunctional, non-exhausted effector T cells, tumor escape was seen in animals treated with STING-vaccine and anti-OX40. The high functionality of the infiltrating T cells and decreased frequency of FoxP3+ CD4+ T cells suggests that immune suppression mechanisms are not responsible for tumor escape; rather, reduced immunogenicity of the tumor is likely occurring. It is possible that loss of MHCI expression by the tumor resulted in an environment where although effector T cells were present, they could not bind to and induce lysis of tumors. Another possibility is that immune-editing of the tumor resulted in outgrowth of tumor cells without expression of the T cell receptor-reactive antigens, however vaccination with peptides corresponding to 12 different, expressed Panc02 antigens makes it unlikely that this was the cause of tumor escape. While we analyzed T cells for expression of exhaustion markers, we did not analyze the tumor itself for the presence of markers of adaptive resistance. The lack of PD-1 on the surface of the infiltrating T cells indicates that PD-L1 expression was not the cause of tumor escape. It has been reported that down-regulation of interferon-alpha receptors on the surface of the tumor can lead to immune evasion in a PD-L1-independent fashion (Benci et al., 2016), and it is possible that this mechanism is occurring in our model.

The decreased frequency of FoxP3+ CD4+ T cells and the presence of a tumor-specific interferon-gamma secreting CD4+ T cell population in STING-vaccine, anti-OX40 treated mice suggests that STING is synergizing with agonist OX40 therapy to skew the CD4+ T cell compartment to a Th1 phenotype. More studies are required to verify this, but if true it would indicate that immunization with peptides specific for both CD4+ and CD8+ antigens should improve tumor clearance rates. Different tumor models have shown varying requirement for either CD4+ or CD8+ T cells in tumor eradication (Castle et al., 2012; Duan

et al., 2014; Gubin et al., 2014; Snyder et al., 2014; Tran et al., 2014; Carreno et al., 2015; Kreiter et al., 2015). By immunizing with 20mer peptides, both CD4⁺ and CD8⁺ T cells can be targeted. T cell depletion studies are on-going to determine what role the CD4⁺ and CD8⁺ T cell compartments play in STING-vaccine primed anti-tumor response.

Taken together, these data suggest that tumors that do not naturally induce spontaneous T cell immunity do not necessarily lack immunogenic epitopes; rather, that targeted immunization provides a potential approach for converting immunotherapy-resistant tumors into sensitive tumors; and that the full repertoire of vaccine targetable epitopes may be underestimated by evaluating endogenous T cell responses that occur spontaneously in tumor-infiltrating lymphocytes. In addition, limiting vaccine epitopes only to those that are predicted to bind to MHC molecules with high affinity may miss epitopes that are capable of inducing protective anti-tumor effector T cells. While therapeutic vaccination with single, strongly immunogenic mutant neoepitopes has been shown to be effective in tumor clearance, either alone or in combination with immune checkpoint blockade antibodies (Castle et al., 2012; Gubin et al., 2014), this study is the first to demonstrate that immunization with pools of subdominant epitopes to which there is no pre-existing response can be effective in a model of pancreatic cancer. Based on these data, patients whose tumors have lower numbers of mutations should still be considered as candidates for mutant neo-epitope-targeted immunotherapy. Furthermore, these data suggest that neo-epitope-targeted immunization will require the addition of appropriate immune checkpoint inhibitors to induce clinically potent antitumor responses. We hypothesize that the addition of mutant neoepitope vaccination converts a classically non-immunogenic tumor (such as PDA) into a more immunogenic tumor that is highly infiltrated with effector lymphocytes as is commonly

seen in microsatellite-instability-high (MSI-high) colorectal cancers; and that OX40 and PD-1 checkpoint blockade modulates this response to improve the anti-tumor response rate. Just as frameshift mutations in MSI-high cancers give rise to neoepitopes that result in T cell infiltration of the tumor, mutome-specific vaccination activates neoepitope-specific T cells that then infiltrate the pancreatic tumor. Although these epitopes are subdominant and do not naturally induce a spontaneous tumor-reactive CD8⁺ T cell response, a response against them can be triggered by a vaccine. The addition of anti-OX40 and anti-PD1 blocking antibodies further boosts this response, presumably by lowering the threshold for T cell activation (anti-OX40) and preventing an exhausted phenotype of these induced tumor-specific T cells (anti-PD-1). In a classically non-immunogenic lesion (such as PDA) where the immunosuppressive environment generally excludes tumor-reactive CD8⁺ T cells, this approach could show efficacy, particularly when combined with depletion of stromal and suppressive elements.

EXPERIMENTAL PROCEDURES

Cell lines and mice

The highly tumorigenic murine Panc02 cell line (Corbett et al., 1984) was maintained in DMEM (Life Technologies) supplemented with 10% fetal bovine serum (Gemini Bio Products), 1% L-glutamine, and 0.5% Penicillin/Streptomycin (Life Technologies) in a humidified atmosphere at 37°C under 10% CO₂. Male C57BL/6, syngeneic to Panc02, age 6 weeks were purchased from Jackson Laboratories and allowed to acclimate for one week prior to experiments. All mice were housed in pathogen-free conditions and treated in accordance with Institutional Animal Care and Use Committee and American Association of Laboratory Animal Committee approved policies.

Peptides and treatment antibodies

All peptides were synthesized by Peptide 2.0 at 70% purity for initial screening experiments. After initial screening, confirmed immunogenic peptides were then synthesized at 95% purity for all further experiments. Lyophilized peptides were stored at 4°C with CaSO₄ dessicant (Drierite) until needed for experiments, then dissolved in DMSO at 50 mg/mL, aliquoted, and stored at -80°C. Once thawed, peptide solutions were kept for no more than 1 month at 4°C. Therapeutic and depletion antibodies were purchased from BioXCell. For checkpoint blockade studies, αPD-1 (100 µg per injection, clone RMP1-14), its isotype control (rat IgG2a, clone 2A3), αOX40 (150 µg per injection, clone OX86), or its isotype control (rat IgG1, clone HRPM) were used. All antibodies were injected intraperitoneally (i.p.) in 200 µL PBS.

Sequencing of tumors

Library preparation and sequencing were performed as described in (Kim et al., 2014) by the Vogelstein group. Secondary analysis was performed on the provided raw sequencing files using the pipeline provided in the git repository https://github.com/rosgood/Panc02_Variant_ID. Briefly, tumor and normal sequences were

aligned by bowtie2, variants called by freebayes with variants with probability less than 0.01 likelihood of not being polymorphic passed to downstream analysis. Variants were then annotated and converted to protein sequences by annovar, peptide 20mer sequences extracted by R, and then a locally maintained NetMHC 3.4 software package was used to predict immunogenicity. All mutations were manually validated using IGV.

Identification of immunogenic mutations

The NetMHC algorithms version 3.2, 3.4, and pan2.8(Lundegaard et al., 2008; Hoof et al., 2009) were used for immunogenicity predictions. Predicted epitopes of lengths 8-11 amino acids containing the identified non-synonymous variants were analyzed for affinity to the H-2Db and H-2Kb MHC I molecules. Corresponding 20mer peptides with mutations centered at position 11 were synthesized by Peptide 2.0 for epitopes with predictions of less than 1000 nM by any of the 3 prediction algorithms. Groups consisted of 3 mice, each mouse receiving 10 µg of the known H-2Kb-binding ovalbumin152-171 peptide

GLEQLESIINFELKLTETSS, a pool of 5-6 peptides at 10 µg per peptide and combined with 10 µg of poly I:C as adjuvant (InVivoGen) in PBS. Mice were immunized with 100 µL in the lower hind limb. 7 days later mice were boosted with identical vaccine formulation. CD8+ T cell responses were measured 7 days after the boost dose by IFN γ ELISPOT as described previously (Thomas et al., 2004). 20mer peptides from LCMV GP133-52 (IITSIKAVYNFATMGILALI) and Trp2175-194 (QIANCSVYDFFVWLHYYSVR) which are known to bind H-2Db and H-2Kb, respectively, were used as controls for background IFN γ secretion.

T cell isolation and ELISpot

CD8+ T cells were isolated from freshly harvested splenocytes by first creating a single-cell suspension by forcing through a 40 µm filter in CTL (RPMI with 10% FBS, 0.5% L-glutamine, 1% Penicillin/Streptomycin, and 0.05 mM 2-mercaptoethanol). Erythrocytes were removed by ACK lysis and resulting lymphocytes were washed, counted and isolated using

the Dynal CD8 negative-isolation kit (Dynal, Invitrogen, Carlsbad, CA, USA) according to manufacturer's instructions. Multiscreen 96-well filtration plates (Millipore) were coated overnight at 4°C with 100 µL/well of 100 µg/mL anti-mouse IFN γ mAb AN18 (Mabtech). Wells were washed three times each with PBS and blocked for 2 hours with CTL media at 37°C. 1×10^5 T2 APCs were pulsed with 2 µg peptide in 100 µL CTL media for 2 hours at 37°C, 5% CO₂. After T cell isolation, 1×10^5 CD8⁺ T cells were added to the capture plate in 100 µL CTL, the T2 APCs with peptide were added, and the plate was incubated for 18 hours at 37°C at 5% CO₂. Cells were removed from the plate by washing 6 times, 2 minutes per wash with PBS + 0.05% Tween20 (Sigma-Aldrich). Wells were incubated for 2 hours at room temperature with 10 µg/mL biotinylated anti-mouse IFN γ mAb R4-6A2 (Mabtech) in 0.05% FBS diluted in PBS. Wells were washed as before, incubated with avidin peroxidase complex (Vectastain ELITE ABS kit; Vector Laboratories) for 1 hour at room temperature, and washed again. AEC substrate was added and well were developed for 10-15 mins at room temperature. The reaction was stopped with tap water and plates were allowed to dry for 24 hours before they were counted using an automated image ELISpot reader (ImmunoSpot).

TIL isolation

Tumors were excised immediately after mice were euthanized and placed into CTL media. Tumors were diced into small pieces and incubated with digestion media (DMEM, 25 mg/L Hyaluronidase, 1 g/L Collagenase IV; Life Technologies), incubated at 37°C for 30 minutes with shaking, and then centrifuged for 10 minutes at 1700 rpm. Tumor samples were washed once with RPMI (Life Technologies), filtered through a 70 µm filter (Falcon), and plated for 1 hour at 37°C, 5% CO₂ to remove adherent tumor cells.

Intracellular cytokine staining and flow cytometry

Isolated cells were stimulated overnight (16 hours) with peptide or anti-CD3/28 magnetic beads (Gibco) in the presence of protein transport inhibitor cocktail (eBioscience). The

following day, cells were washed with PBS, stained with Live/Dead Fixable aqua (Life Technologies) for 20 minutes on ice in the dark, washed 3 times with PBS, then stained for surface markers diluted in FACS buffer (PBS with 1% FBS and 0.1% NaN_3) for 30 minutes on ice in the dark. Cells were washed 3 times with FACS buffer, fixed and permeabilized using a FoxP3 Fix/Perm kit (eBioscience) for 20 minutes at room temperature in the dark. Cells were then washed once with Perm/Wash buffer and stained for intracellular markers. After washing 3 times, cells were resuspended in FACS buffer and either run on a Gallios flow cytometer (Beckman Coulter) immediately or after overnight storage at 4°C in the dark. Analysis was performed using FlowJo (Treestar).

Antitumor models

For antitumor experiments, mice received a subcutaneous injection of 1×10^6 Panc02 cells in 0.1 mL sterile PBS in the inner flank of the right hind limb on day 0. Tumor measurements were taken twice weekly beginning on day 10 and tumor volume was calculated as length multiplied by width squared divided by 2. Mice were sacrificed when tumors reached 1 cm³, began to impede mobility, or began to ulcerate. At this time, spleens and tumors were harvested for ELISpot, flow cytometry, or immunofluorescence as described previously. Peptide vaccine was given on days 3 and 10 and consisted of the 14 expressed immunogenic peptides in table 1 (50 µg each) with 10 µg of poly I:C in 100 µL of sterile PBS per mouse. Vaccination was performed subcutaneously at the base of the tail. For checkpoint blockade experiments, tumor injections were performed as with T cell depletion studies, but treatment was delayed until tumors were palpable, at day 10.

Statistical Analysis

Statistical analysis was performed using GraphPad Prism software. All data is presented as mean \pm standard error (SEM). For survival curve analysis, the log-rank (Mantel-Cox) test was used.

REFERENCES

Ascarateil S, Puget A, Koziol M-E (2015): Safety data of Montanide ISA 51 VG and Montanide ISA 720 VG, two adjuvants dedicated to human therapeutic vaccines. *Journal for ImmunoTherapy of Cancer*, 3, P428. doi:10.1186/2051-1426-3-S2-P428.

Aucouturier J, Dupuis L, Deville S, Ascarateil S, Ganne V (2002): Montanide ISA 720 and 51: a new generation of water in oil emulsions as adjuvants for human vaccines. *Expert review of vaccines*, 1, 111–118. doi:10.1586/14760584.1.1.111.

Aucouturier J, Dupuis L, Ganne V (2001): Adjuvants designed for veterinary and human vaccines. *Vaccine*, 19, 2666–2672. doi:10.1016/S0264-410X(00)00498-9.

Baird JR, Friedman D, Cottam B, Dubensky TW, Kanne DB, Bambina S, Bahjat K, Crittenden MR, Gough MJ (2016): Radiotherapy Combined with Novel STING-Targeting Oligonucleotides Results in Regression of Established Tumors. *Cancer Research*, 76, 50–61. doi:10.1158/0008-5472.CAN-14-3619.

Benci JL, Xu B, Qiu Y, Wu TJ, Dada H, Twyman-Saint Victor C, Cucolo L, Lee DSM, Pauken KE, Huang AC, Gangadhar TC, Amaravadi RK, Schuchter LM, Feldman MD, Ishwaran H, Vonderheide RH, Maity A, Wherry EJ, Minn AJ (2016): Tumor Interferon Signaling Regulates a Multigenic Resistance Program to Immune Checkpoint Blockade. *Cell*, 167, 1540–1554.e12. doi:10.1016/j.cell.2016.11.022.

Black CM, Armstrong TD, Jaffee EM (2014): Apoptosis-Regulated Low-Avidity Cancer-

Specific CD8⁺ T Cells Can Be Rescued to Eliminate HER2/neu-Expressing Tumors by Costimulatory Agonists in Tolerized Mice. *Cancer Immunology Research*, 2, 307–319. doi:10.1158/2326-6066.CIR-13-0145.

Brahmer JR, Drake CG, Wollner I, Powderly JD, Picus J, Sharfman WH, Stankevich E, Pons A, Salay TM, McMiller TL, Gilson MM, Wang C, Selby M, Taube JM, Anders R, Chen L, Korman AJ, Pardoll DM, Lowy I, Topalian SL (2010): Phase I Study of Single-Agent Anti-Programmed Death-1 (MDX-1106) in Refractory Solid Tumors: Safety, Clinical Activity, Pharmacodynamics, and Immunologic Correlates. *Journal of Clinical Oncology*, 28, 3167–3175. doi:10.1200/JCO.2009.26.7609.

Brahmer JR, Tykodi SS, Chow LQM, Hwu W-J, Topalian SL, Hwu P, Drake CG, Camacho LH, Kauh J, Odunsi K, Pitot HC, Hamid O, Bhatia S, Martins R, Eaton K, Chen S, Salay TM, Alaparthi S, Grosso JF, Korman AJ, Parker SM, Agrawal S, Goldberg SM, Pardoll DM, Gupta A, Wigginton JM (2012): Safety and Activity of Anti-PD-L1 Antibody in Patients with Advanced Cancer. *New England Journal of Medicine*, 366, 2455–2465. doi:10.1056/NEJMoa1200694.

Calabro S, Tritto E, Pezzotti A, Taccone M, Muzzi A, Bertholet S, De Gregorio E, O'Hagan DT, Baudner B, Seubert A (2013): The adjuvant effect of MF59 is due to the oil-in-water emulsion formulation, none of the individual components induce a comparable adjuvant effect. *Vaccine*, 31, 3363–3369. doi:10.1016/j.vaccine.2013.05.007.

Carreno BM, Magrini V, Becker-Hapak M, Kaabinejadian S, Hundal J, Petti AA, Ly A, Lie W-R, Hildebrand WH, Mardis ER, Linette GP (2015): Cancer immunotherapy. A dendritic

cell vaccine increases the breadth and diversity of melanoma neoantigen-specific T cells. *Science*, 348, 803–808. doi:10.1126/science.aaa3828.

Castle JC, Kreiter S, Diekmann J, Lower M, van de Roemer N, de Graaf J, Selmi A, Diken M, Boegel S, Paret C, Koslowski M, Kuhn AN, Britten CM, Huber C, Tureci O, Sahin U (2012): Exploiting the Mutanome for Tumor Vaccination. *Cancer Research*, 72, 1081–1091. doi:10.1158/0008-5472.CAN-11-3722.

Celis E (2007): Toll-like receptor ligands energize peptide vaccines through multiple paths. *Cancer Research*, 67, 7945–7947. doi:10.1158/0008-5472.CAN-07-1652.

Colombo MP, Piconese S (2007): Regulatory T-cell inhibition versus depletion: the right choice in cancer immunotherapy. *Nature Reviews Cancer*, 7, 880–887. doi:10.1038/nrc2250.

Corbett TH, Roberts BJ, Leopold WR, Peckham JC, Wilkoff LJ, Griswold DP, Schabel FM (1984): Induction and chemotherapeutic response of two transplantable ductal adenocarcinomas of the pancreas in C57BL/6 mice. *Cancer Research*, 44, 717–726.

Currie AJ, van der Most RG, Broomfield SA, Prosser AC, Tovey MG, Robinson BWS (2008): Targeting the effector site with IFN- α -inducing TLR ligands reactivates tumor-resident CD8 T cell responses to eradicate established solid tumors. *Journal of immunology (Baltimore, Md : 1950)*, 180, 1535–1544. doi:10.4049/jimmunol.180.3.1535.

Duan F, Duitama J, Seesi AI S, Ayres CM, Corcelli SA, Pawashe AP, Blanchard T, McMahon D, Sidney J, Sette A, Baker BM, Mandoiu II, Srivastava PK (2014): Genomic and bioinformatic profiling of mutational neoepitopes reveals new rules to predict anticancer

immunogenicity. *Journal of Experimental Medicine*, 12, R18.

doi:10.1107/S0907444904013587.

Emens LA (2005): Breast cancer vaccines: maximizing cancer treatment by tapping into host immunity. *Endocrine Related Cancer*, 12, 1–17. doi:10.1677/erc.1.00671.

Flies DB, Chen L (2007): The new B7s: playing a pivotal role in tumor immunity. *Journal of Immunotherapy*, 30, 251–260. doi:10.1097/CJI.0b013e31802e085a.

Fu J, Kanne DB, Leong M, Glickman LH, McWhirter SM, Lemmens E, Mechette K, Leong JJ, Lauer P, Liu W, Sivick KE, Zeng Q, Soares KC, Zheng L, Portnoy DA, Woodward JJ, Pardoll DM, Dubensky TW, Kim Y (2015): STING agonist formulated cancer vaccines can cure established tumors resistant to PD-1 blockade. *Science Translational Medicine*, 7, 283ra52–283ra52. doi:10.1126/scitranslmed.aaa4306.

Garrison E, Marth G (2012): Haplotype-based variant detection from short-read sequencing. *arXivorg*, q-bio.GN.

Gubin MM, Zhang X, Schuster H, Caron E, Ward JP, Noguchi T, Ivanova Y, Hundal J, Arthur CD, Krebber W-J, Mulder GE, Toebes M, Vesely MD, Lam SSK, Korman AJ, Allison JP, Freeman GJ, Sharpe AH, Pearce EL, Schumacher TN, Aebersold R, Rammensee H-G, Melief CJM, Mardis ER, Gillanders WE, Artyomov MN, Schreiber RD (2014): Checkpoint blockade cancer immunotherapy targets tumour-specific mutant antigens. *Nature*, 515, 577–581. doi:10.1038/nature13988.

Guo Z, Wang X, Cheng D, Xia Z, Luan M, Zhang S (2014): PD-1 blockade and OX40

triggering synergistically protects against tumor growth in a murine model of ovarian cancer. PloS one, 9, e89350. doi:10.1371/journal.pone.0089350.

Hirschhorn-Cymerman D, Rizzuto GA, Merghoub T, Cohen AD, Avogadri F, Lesokhin AM, Weinberg AD, Wolchok JD, Houghton AN (2009): OX40 engagement and chemotherapy combination provides potent antitumor immunity with concomitant regulatory T cell apoptosis. Journal of Experimental Medicine, 206, 1103–1116. doi:10.1084/jem.20082205.

Hoof I, Peters B, Sidney J, Pedersen LE, Sette A, Lund O, Buus S, Nielsen M (2009): NetMHCpan, a method for MHC class I binding prediction beyond humans. Immunogenetics, 61, 1–13. doi:10.1007/s00251-008-0341-z.

Hugo W, Zaretsky JM, Sun L, Song C, Moreno BH, Hu-Lieskovan S, Berent-Maoz B, Pang J, Chmielowski B, Cherry G, Seja E, Lomeli S, Kong X, Kelley MC, Sosman JA, Johnson DB, Ribas A, Lo RS (2016): Genomic and Transcriptomic Features of Response to Anti-PD-1 Therapy in Metastatic Melanoma. Cell, 165, 35–44. doi:10.1016/j.cell.2016.02.065.

Jones S, Zhang X, Parsons DW, Lin JCH, Leary RJ, Angenendt P, Mankoo P, Carter H, Kamiyama H, Jimeno A, Hong SM, Fu B, Lin MT, Calhoun ES, Kamiyama M, Walter K, Nikolskaya T, Nikolsky Y, Hartigan J, Smith DR, Hidalgo M, Leach SD, Klein AP, Jaffee EM, Goggins M, Maitra A, Iacobuzio-Donahue C, Eshleman JR, Kern SE, Hruban RH, Karchin R, Papadopoulos N, Parmigiani G, Vogelstein B, Velculescu VE, Kinzler KW (2008): Core Signaling Pathways in Human Pancreatic Cancers Revealed by Global Genomic Analyses. Science, 321, 1801–1806. doi:10.1126/science.1164368.

Kim K, Skora AD, Li Z, Liu Q, Tam AJ, Blosser RL, Diaz LA, Papadopoulos N, Kinzler

KW, Vogelstein B, Zhou S (2014): Eradication of metastatic mouse cancers resistant to immune checkpoint blockade by suppression of myeloid-derived cells. *Proceedings of the National Academy of Sciences*, 111, 11774–11779. doi:10.1073/pnas.1410626111.

Kreiter S, Vormehr M, van de Roemer N, Diken M, Löwer M, Diekmann J, Boegel S, Schrörs B, Vascotto F, Castle JC, Tadmor AD, Schoenberger SP, Huber C, Türeci Ö, Sahin U (2015): Mutant MHC class II epitopes drive therapeutic immune responses to cancer. *Nature*, 520, 692–696. doi:10.1038/nature14426.

Kvistborg P, Philips D, Kelderman S, Hageman L, Ottensmeier C, Joseph-Pietras D, Welters MJP, van der Burg S, Kapiteijn E, Michielin O, Romano E, Linnemann C, Speiser D, Blank C, Haanen JB, Schumacher TN (2014): Anti-CTLA-4 therapy broadens the melanoma-reactive CD8+ T cell response. *Science Translational Medicine*, 6, 254ra128–254ra128. doi:10.1126/scitranslmed.3008918.

Langmead B, Salzberg SL (2012): Fast gapped-read alignment with Bowtie 2. *Nature Methods*, 9, 357–359. doi:10.1038/nmeth.1923.

Le DT, Uram JN, Wang H, Bartlett BR, Kemberling H, Eyring AD, Skora AD, Luber BS, Azad NS, Laheru D, Biedrzycki B, Donehower RC, Zaheer A, Fisher GA, Crocenzi TS, Lee JJ, Duffy SM, Goldberg RM, la Chapelle de A, Koshiji M, Bhaijee F, Huebner T, Hruban RH, Wood LD, Cuka N, Pardoll DM, Papadopoulos N, Kinzler KW, Zhou S, Cornish TC, Taube JM, Anders RA, Eshleman JR, Vogelstein B, Diaz LA Jr. (2015): PD-1 Blockade in Tumors with Mismatch-Repair Deficiency. *New England Journal of Medicine*, 372, 2509–2520. doi:10.1056/NEJMoa1500596.

Linette GP, Stadtmauer EA, Maus MV, Rapoport AP, Levine BL, Emery L, Litzky L, Bagg A, Carreno BM, Cimino PJ, Binder-Scholl GK, Smethurst DP, Gerry AB, Pumphrey NJ, Bennett AD, Brewer JE, Dukes J, Harper J, Tayton-Martin HK, Jakobsen BK, Hassan NJ, Kalos M, June CH (2013): Cardiovascular toxicity and titin cross-reactivity of affinity-enhanced T cells in myeloma and melanoma. *Blood*, 122, 863–871. doi:10.1182/blood-2013-03-490565.

Lipson EJ, Sharfman WH, Drake CG, Wollner I, Taube JM, Anders RA, Xu H, Yao S, Pons A, Chen L, Pardoll DM, Brahmer JR, Topalian SL (2013): Durable Cancer Regression Off-Treatment and Effective Reinduction Therapy with an Anti-PD-1 Antibody. *Clinical Cancer Research*, 19, 462–468. doi:10.1158/1078-0432.CCR-12-2625.

Lundegaard C, Lund O, Nielsen M (2008): Accurate approximation method for prediction of class I MHC affinities for peptides of length 8, 10 and 11 using prediction tools trained on 9mers. *Bioinformatics (Oxford, England)*, 24, 1397–1398. doi:10.1093/bioinformatics/btn128.

Melief CJ (2009): Immunotherapy of Cancer by Vaccination with Long Syn-thetic Peptides. *Journal of Medical Sciences*, 2, 43–45.

Moore E, Clavijo PE, Davis R, Cash H, Van Waes C, Kim Y, Allen C (2016): Established T Cell-Inflamed Tumors Rejected after Adaptive Resistance Was Reversed by Combination STING Activation and PD-1 Pathway Blockade. *Cancer Immunology Research*, 4, 1061–1071. doi:10.1158/2326-6066.CIR-16-0104.

Murata S, Ladle BH, Kim PS, Lutz ER, Wolpoe ME, Ivie SE, Smith HM, Armstrong TD,

Emens LA, Jaffee EM, Reilly RT (2006): OX40 Costimulation Synergizes with GM-CSF Whole-Cell Vaccination to Overcome Established CD8⁺ T Cell Tolerance to an Endogenous Tumor Antigen. *Journal of immunology* (Baltimore, Md : 1950), 176, 974–983.

doi:10.4049/jimmunol.176.2.974.

Nomi T, Sho M, Akahori T, Hamada K, Kubo A, Kanehiro H, Nakamura S, Enomoto K, Yagita H, Azuma M, Nakajima Y (2007): Clinical Significance and Therapeutic Potential of the Programmed Death-1 Ligand/Programmed Death-1 Pathway in Human Pancreatic Cancer. *Clinical Cancer Research*, 13, 2151–2157. doi:10.1158/1078-0432.CCR-06-2746.

Ohigashi Y, Sho M, Yamada Y, Tsurui Y, Hamada K, Ikeda N, Mizuno T, Yoriki R, Kashizuka H, Yane K, Tsushima F, Otsuki N, Yagita H, Azuma M, Nakajima Y (2005): Clinical significance of programmed death-1 ligand-1 and programmed death-1 ligand-2 expression in human esophageal cancer. *Clinical cancer research : an official journal of the American Association for Cancer Research*, 11, 2947–2953. doi:10.1158/1078-0432.CCR-04-1469.

Ott G, Barchfeld GL, Chernoff D, Radhakrishnan R, van Hoogevest P, Van Nest G (1995): MF59. Design and evaluation of a safe and potent adjuvant for human vaccines. *Pharmaceutical biotechnology*, 6, 277–296.

Ott G, Radhakrishnan R, Fang J-H, Hora M (2000): The Adjuvant MF59: A 10-Year Perspective In: *Vaccine Adjuvants*. Humana Press, New Jersey, pp. 211–228.

Pulko V, Liu X, Krco CJ, Harris KJ, Frigola X, Kwon ED, Dong H (2009): TLR3-stimulated dendritic cells up-regulate B7-H1 expression and influence the magnitude of CD8 T cell responses to tumor vaccination. *The Journal of Immunology*, 183, 3634–3641.

doi:10.4049/jimmunol.0900974.

R Core Team (2016): R: A Language and Environment for Statistical Computing. R Foundation for Statistical Computing, Vienna, Austria.

Rizvi NA, Hellmann MD, Snyder A, Kvistborg P, Makarov V, Havel JJ, Lee W, Yuan J, Wong P, Ho TS, Miller ML, Rekhtman N, Moreira AL, Ibrahim F, Bruggeman C, Gasmi B, Zappasodi R, Maeda Y, Sander C, Garon EB, Merghoub T, Wolchok JD, Schumacher TN, Chan TA (2015): Cancer immunology. Mutational landscape determines sensitivity to PD-1 blockade in non-small cell lung cancer. *Science*, 348, 124–128. doi:10.1126/science.aaa1348.

Robinson JT, Thorvaldsdóttir H, Winckler W, Guttman M, Lander ES, Getz G, Mesirov JP (2011): Integrative genomics viewer. *Nature Biotechnology*, 29, 24–26. doi:10.1038/nbt0111-24.

Ruby CE, Yates MA, Hirschhorn-Cymerman D, Chlebeck P, Wolchok JD, Houghton AN, Offner H, Weinberg AD (2009): Cutting Edge: OX40 agonists can drive regulatory T cell expansion if the cytokine milieu is right. *The Journal of Immunology*, 183, 4853–4857. doi:10.4049/jimmunol.0901112.

Salem ML, Kadima AN, Cole DJ, Gillanders WE (2005): Defining the Antigen-Specific T-Cell Response to Vaccination and Poly(I:C)/TLR3 Signaling. *Journal of Immunotherapy*, 28, 220–228. doi:10.1097/01.cji.0000156828.75196.0d.

Siegel RL, Miller KD, Jemal A (2016): Cancer statistics, 2016. *CA: A Cancer Journal for Clinicians*, 66, 7–30. doi:10.3322/caac.21332.

Snyder A, Makarov V, Merghoub T, Yuan J, Zaretsky JM, Desrichard A, Walsh LA, Postow MA, Wong P, Ho TS, Hollmann TJ, Bruggeman C, Kannan K, Li Y, Elipenahli C, Liu C, Harbison CT, Wang L, Ribas A, Wolchok JD, Chan TA (2014): Genetic Basis for Clinical Response to CTLA-4 Blockade in Melanoma. *New England Journal of Medicine*, 371, 2189–2199. doi:10.1056/NEJMoa1406498.

Soares KC, Rucki AA, Wu AA, Olino K, Xiao Q, Chai Y, Wamwea A, Bigelow E, Lutz E, Liu L, Yao S, Anders RA, Laheru D, Wolfgang CL, Edil BH, Schulick RD, Jaffee EM, Zheng L (2015): PD-1/PD-L1 blockade together with vaccine therapy facilitates effector T-cell infiltration into pancreatic tumors. *Journal of immunotherapy (Hagerstown, Md : 1997)*, 38, 1–11. doi:10.1097/CJI.0000000000000062.

Thomas AM, Santarsiero LM, Lutz ER (2004): Mesothelin-specific CD8+ T Cell Responses Provide Evidence of In Vivo Cross-Priming by Antigen-Presenting Cells in Vaccinated Pancreatic Cancer Patients. *Journal of Experimental Medicine*, 200, 297–306. doi:10.1084/jem.20031435.

Thompson RH, Kuntz SM, Leibovich BC, Dong H, Lohse CM, Webster WS, Sengupta S, Frank I, Parker AS, Zincke H, Blute ML, Sebo TJ, Cheville JC, Kwon ED (2006): Tumor B7-H1 Is Associated with Poor Prognosis in Renal Cell Carcinoma Patients with Long-term Follow-up. *Cancer Research*, 66, 3381–3385. doi:10.1158/0008-5472.CAN-05-4303.

Thorvaldsdottir H, Robinson JT, Mesirov JP (2013): Integrative Genomics Viewer (IGV): high-performance genomics data visualization and exploration. *Briefings in Bioinformatics*, 14, 178–192. doi:10.1093/bib/bbs017.

Topalian SL, Hodi FS, Brahmer JR, Gettinger SN, Smith DC, McDermott DF, Powderly JD, Carvajal RD, Sosman JA, Atkins MB, Leming PD, Spigel DR, Antonia SJ, Horn L, Drake CG, Pardoll DM, Chen L, Sharfman WH, Anders RA, Taube JM, McMiller TL, Xu H, Korman AJ, Jure-Kunkel M, Agrawal S, McDonald D, Kollia GD, Gupta A, Wigginton JM, Sznol M (2012): Safety, activity, and immune correlates of anti-PD-1 antibody in cancer. *New England Journal of Medicine*, 366, 2443–2454. doi:10.1056/NEJMoa1200690.

Tran E, Turcotte S, Gros A, Robbins PF, Lu YC, Dudley ME, Wunderlich JR, Somerville RP, Hogan K, Hinrichs CS, Parkhurst MR, Yang JC, Rosenberg SA (2014): Cancer Immunotherapy Based on Mutation-Specific CD4⁺ T Cells in a Patient with Epithelial Cancer. *Science*, 344, 641–645. doi:10.1126/science.1251102.

Uram JN, Black CM, Flynn E, Huang L, Armstrong TD, Jaffee EM (2011): Nondominant CD8 T Cells Are Active Players in the Vaccine-Induced Antitumor Immune Response. *The Journal of Immunology*, 186, 3847–3857. doi:10.4049/jimmunol.1000361.

Van Allen EM, Miao D, Schilling B, Shukla SA, Blank C, Zimmer L, Sucker A, Hillen U, Foppen MHG, Goldinger SM, Utikal J, Hassel JC, Weide B, Kaehler KC, Loquai C, Mohr P, Gutzmer R, Dummer R, Gabriel S, Wu CJ, Schadendorf D, Garraway LA (2015): Genomic correlates of response to CTLA-4 blockade in metastatic melanoma. *Science*, 350, 207–211. doi:10.1126/science.aad0095.

van Rooij N, van Buuren MM, Philips D, Velds A, Toebes M, Heemskerk B, van Dijk LJA, Behjati S, Hilkmann H, Atmioui El D, Nieuwland M, Stratton MR, Kerkhoven RM, Kesmir C, Haanen JB, Kvistborg P, Schumacher TN (2013): Tumor exome analysis reveals

neoantigen-specific T-cell reactivity in an ipilimumab-responsive melanoma. *Journal of Clinical Oncology*, 31, e439–e442. doi:10.1200/JCO.2012.47.7521.

Vogelstein B, Papadopoulos N, Velculescu VE, Zhou S, Diaz LA, Kinzler KW (2013): Cancer Genome Landscapes. *Science*, 339, 1546–1558.

Vu MD, Xiao X, Gao W, Degauque N, Chen M, Kroemer A, Killeen N, Ishii N, Chang Li X (2007): OX40 costimulation turns off Foxp3+ Tregs. *Blood*, 110, 2501–2510. doi:10.1182/blood-2007-01-070748.

Wang K, Li M, Hakonarson H (2010): ANNOVAR: functional annotation of genetic variants from high-throughput sequencing data. *Nucleic Acids Research*, 38, e164–e164. doi:10.1093/nar/gkq603.

Waterston RH, Lindblad-Toh K, Birney E, Rogers J, Abril JF, Agarwal P, Agarwala R, Ainscough R, Alexandersson M, An P, Antonarakis SE, Attwood J, Baertsch R, Bailey J, Barlow K, Beck S, Berry E, Birren B, Bloom T, Bork P, Botcherby M, Bray N, Brent MR, Brown DG, Brown SD, Bult C, Burton J, Butler J, Campbell RD, Carninci P, Cawley S, Chiaromonte F, Chinwalla AT, Church DM, Clamp M, Clee C, Collins FS, Cook LL, Copley RR, Coulson A, Couronne O, Cuff J, Curwen V, Cutts T, Daly M, David R, Davies J, Delehaunty KD, Deri J, Dermitzakis ET, Dewey C, Dickens NJ, Diekhans M, Dodge S, Dubchak I, Dunn DM, Eddy SR, Elnitski L, Emes RD, Eswara P, Eyraes E, Felsenfeld A, Fewell GA, Flicek P, Foley K, Frankel WN, Fulton LA, Fulton RS, Furey TS, Gage D, Gibbs RA, Glusman G, Gnerre S, Goldman N, Goodstadt L, Grafham D, Graves TA, Green ED, Gregory S, Guigo R, Guyer M, Hardison RC, Haussler D, Hayashizaki Y, Hillier LW,

Hinrichs A, Hlavina W, Holzer T, Hsu F, Hua A, Hubbard T, Hunt A, Jackson I, Jaffe DB, Johnson LS, Jones M, Jones TA, Joy A, Kamal M, Karlsson EK, Karolchik D, Kasprzyk A, Kawai J, Keibler E, Kells C, Kent WJ, Kirby A, Kolbe DL, Korf I, Kucherlapati RS, Kulbokas EJ, Kulp D, Landers T, Leger JP, Leonard S, Letunic I, Levine R, Li J, Li M, Lloyd C, Lucas S, Ma B, Maglott DR, Mardis ER, Matthews L, Mauceli E, Mayer JH, McCarthy M, McCombie WR, McLaren S, McLay K, McPherson JD, Meldrim J, Meredith B, Mesirov JP, Miller W, Miner TL, Mongin E, Montgomery KT, Morgan M, Mott R, Mullikin JC, Muzny DM, Nash WE, Nelson JO, Nhan MN, Nicol R, Ning Z, Nusbaum C, O'Connor MJ, Okazaki Y, Oliver K, Larty EO, Pachter L, Parra G, Pepin KH, Peterson J, Pevzner P, Plumb R, Pohl CS, Poliakov A, Ponce TC, Ponting CP, Potter S, Quail M, Reymond A, Roe BA, Roskin KM, Rubin EM, Rust AG, Santos R, Sapojnikov V, Schultz B, Schultz J, Schwartz MS, Schwartz S, Scott C, Seaman S, Searle S, Sharpe T, Sheridan A, Shownkeen R, Sims S, Singer JB, Slater G, Smit A, Smith DR, Spencer B, Stabenau A, Strange-Thomann NS, Sugnet C, Suyama M, Tesler G, Thompson J, Torrents D, Trevaskis E, Tromp J, Ucla C, Vidal AU, Vinson JP, Niederhausern von AC, Wade CM, Wall M, Weber RJ, Weiss RB, Wendl MC, West AP, Wetterstrand K, Wheeler R, Whelan S, Wierzbowski J, Willey D, Williams S, Wilson RK, Winter E, Worley KC, Wyman D, Yang S, Yang SP, Zdobnov EM, Zody MC, Lander ES, Consor MGS (2002): Initial sequencing and comparative analysis of the mouse genome. *Nature*, 420, 520–562. doi:10.1038/nature01262.

Winograd R, Byrne KT, Evans RA, Odorizzi PM, Meyer ARL, Bajor DL, Clendenin C, Stanger BZ, Furth EE, Wherry EJ, Vonderheide RH (2015): Induction of T-cell Immunity Overcomes Complete Resistance to PD-1 and CTLA-4 Blockade and Improves Survival in Pancreatic Carcinoma. *Cancer Immunology Research*, 3, 399–411. doi:10.1158/2326-

6066.CIR-14-0215.

Wu C, Zhu Y, Jiang J, Zhao J, Zhang X-G, Xu N (2006): Immunohistochemical localization of programmed death-1 ligand-1 (PD-L1) in gastric carcinoma and its clinical significance. *Acta Histochemica*, 108, 19–24. doi:10.1016/j.acthis.2006.01.003.

Zou W, Chen L (2008): Inhibitory B7-family molecules in the tumour microenvironment. *Nature Reviews Immunology*, 8, 467–477. doi:10.1038/nri2326.

Heather L. Kinkead

Department of Oncology, Sidney Kimmel Comprehensive Cancer Center
The Johns Hopkins University School of Medicine
1650 Orleans Street, Cancer Research Building 1, Room 422, Baltimore, Maryland 21287
Home: 858-220-6829 Work: 410-614-4772
Email: hkinkeal@jhmi.edu

Ph.D.	2017	Cellular and Molecular Medicine
--------------	-------------	--

Johns Hopkins School of Medicine, Baltimore, Maryland

Dissertation: Subdominant epitopes in combination with checkpoint blockade modulators are protective in a model of pancreatic adenocarcinoma

Advisor: Elizabeth M. Jaffee, M.D.

B.S. 2006 Molecular Biology

University of California, San Diego, La Jolla, California

Johns Hopkins School of Medicine; Baltimore, MD — August 2012-March 2017

Ph.D. Candidate, Jaffee Laboratory

Utilization of the STING pathway to optimally prime a tumor-specific T cell response, combining neoantigen and shared antigen targeting with checkpoint blockade to induce a productive anti-tumor response

- Identification of non-synonymous mutations present in tumors from whole exome sequencing data
- Predicted binding affinities of mutome-derived peptides for MHC class I using NetMHC algorithms
- *In vivo* immunizations and ELISpot analysis to determine T cell reactivity
- Flow cytometry analysis of tumor-infiltrating and peripheral cell populations
- Immunofluorescence of tumor sections

Genomics Institute of the Novartis Foundation; La Jolla, CA — June 2011-July 2012

Scientific Associate, Biotherapeutics Division

- Production of monoclonal antibodies by mammalian cell transfection
- Cell-based assays to test function of biologics
- Assessing affinity of proteins by ELISA, Bio-Layer Interferometry, and FACS
- Isolation and culturing of primary cells
- Literature research of potential therapeutic targets

The Scripps Research Institute; La Jolla, CA — October 2009-June 2011

Research Assistant, Mosier Laboratory

- Isolation and analysis of RNA transcripts from primary cells by real-time PCR
- Culturing and infecting of primary cells and cell lines with replication-competent and pseudoviral HIV-1 in BSL-3 and BSL-2/3 facilities
- Isolation and culturing of primary cells from human donors

- Viral RNA rescue and subsequent cDNA synthesis and cloning from cell culture supernatants
- Expression and purification of recombinant proteins from mammalian and bacterial cell cultures

The Scripps Research Institute; La Jolla, CA — June 2006-October 2009

Research Assistant, Burton/Zwick Laboratories

- Created and characterized HIV-1 viral envelopes by heat stability, neutralization profile, antibody capture, and PAGE/western blot analysis
- Created, screened and characterized antibody libraries for affinity maturation using phage display, yeast display, and FACS
- Expressed, purified, and characterized recombinant proteins from *E. coli* by ELISA

Pharmexa-Epimmune; San Diego, CA — September 2005-May 2006

Student Assistant, Vaccine Development

- Created plasmid vectors using PCR, agarose gel electrophoresis, gel purification, and restriction digest
- Employed aseptic tissue culture technique to maintain immortalized cell lines
- Performed ELISpot assays for detection and quantification of activated T-cells from mouse splenocytes
- Performed mouse injections to investigate T-cell activation

Publications and Presentations

Kinkead H, Jaffee EM, Lutz ER & Armstrong, TD. Vaccines and Their Role in CD8 T Cell-Mediated Antitumor Immunity, in *Encyclopedia of Immunobiology* 534–541 (Elsevier, 2016)

Kinkead H, Jaffee EM, Lutz ER. Exploiting the Pancreatic Cancer Mutome. Presented at: *Keystone Symposia Tumor Immunology: Multidisciplinary Science Driving Combination Therapy* J7:2024 (2015)

Lutz ER, **Kinkead H**, Jaffee EM & Zheng L. Priming the pancreatic cancer tumor microenvironment for checkpoint-inhibitor immunotherapy. *Oncoimmunology* 3, e962401 (2014)

Lutz E, **Kinkead H**, Yager A, Armstrong T, Lauer P, Brockstedt D, Dubensky T, Jaffee E. Development of mutome-specific personalized vaccines for pancreatic cancer. *Journal for ImmunoTherapy of Cancer* 1, P224 (2013)

Agrawal N, Leaman D, Rowcliffe E, **Kinkead H**, Nohria R, Akagi J, Bauer K, Du S, Whalen R, Burton D, Zwick, M. Functional Stability of Unliganded Envelope Glycoprotein Spikes among Isolates of Human Immunodeficiency Virus Type 1 (HIV-1). *PLoS ONE* 6, e21339 (2011)

Leaman DP, **Kinkead H**, Zwick MB. In-solution virus capture assay helps deconstruct heterogeneous antibody recognition of human immunodeficiency virus type 1. *J Virol*.

84:3382-95 (2010)

Nelson JD*, **Kinkead H***, Brunel F, Leaman DP, Jensen R, Louis JM, Maruyama T, Bewley C, Bowdish K, Clore GM, Dawson PE, Frederickson S, Mage RG, Richman DD, Burton DR, Zwick MB. Antibody elicited against the gp41 N-heptad repeat (NHR) coiled-coil can neutralize HIV-1 with modest potency but non-neutralizing antibodies also bind to NHR mimetics. *Virology* 377(1):170-83 (2008) *co-first author

Society memberships

- **Federation of Clinical Immunology Societies, 2013-2017**
- **American Association for Cancer Research, 2017**

Additional skills and interests

Contributing author to Open Science DB, dedicated to translating current research articles into common language for the general public.

Contributing author to Federation of Clinical Immunology Societies Translational Immunology Update 2014-2015, providing article summaries of cutting edge immunology research.

Software

GraphPad Prism, FlowJo, Kaluza, Samtools, Annovar, Integrated Genomics Viewer, Genome Analysis ToolKit (GATK), Applied Biosystems SDS 2.4, PrimerExpress Real-Time PCR Design Software, DNASTar Lasergene, PyMOL, ImageJ, Microsoft Office

References

Elizabeth M. Jaffee, M.D.
The Dana and Albert “Cubby” Broccoli Professor of Oncology
Deputy Director, The Sidney Kimmel Comprehensive Cancer Center at Johns Hopkins
Co-Director, Gastrointestinal Cancer Program
The Johns Hopkins University School of Medicine
1650 Orleans Street, CRB1, 4M07
Baltimore, MD 21287
Email: ejaffee@jhmi.edu
Phone: 410-955-2957

Eric R. Lutz, Ph.D.
Senior Principal Scientist, WindMIL Therapeutics Inc.
WindMIL Therapeutics Inc.
855 N. Wolf Street
Baltimore, MD 21205
Email: lutz@windmiltherapeutics.com
Phone: 410-908-7701